INNOVATION FOREVER
Open Access

Innovation Discovery

ISSN 2959-5150 (Online)

Research Article

Structural Analysis of Polylactic Acid in Composite Starch Biopolymers – A Stochastic Dynamics Mass Spectrometric Approach

Bojidarka Ivanova[1*]

[1]*Lehrstuhl für Analytische Chemie, Institut für Umweltforschung, Fakultät für Chemie und Chemische Biologie, Technische Universität Dortmund, Dortmund, Germany*

[*]***Correspondence to: Bojidarka Ivanova, PhD, Associate Professor,*** *Lehrstuhl für Analytische Chemie, Institut für Umweltforschung, Fakultät für Chemie und Chemische Biologie, Technische Universität Dortmund, Otto-Hahn-Straße 6, Dortmund, 44221, Nordrhein-Westfalen, Germany; Email: bojidarka.ivanova@yahoo.com*

Abstract

Since, by 2050 at about 12 thousand metric tons waste of synthetic plastics shall pollute the environment, and only 9% of them have been recycled, there is position involving synthetic plastics replacement with carbohydrates-based eco-friendly bioplastics such as cellulose, starch and polylactic acid (PLA) obtained via starch fermentation. Biodegradable polymers could contain toxic chemicals, however, and there is central issue to assess risk to human health and environment from polymers due to chemical exposure of bioplastics food packing by exact methods for determining chemicals and molecular structure of polymers. Mass spectrometry, due to superior performances occupied irreplaceable place in environmental research and food technologies. It faces, however, challenge in determining carbohydrate 3D molecular structures. This study solves the problem using innovative stochastic dynamics equations for exact data-processing of mass spectrometric measurable variables. It analyses PLA in starch and cellulose bioplastics of single-use drinking cups, films and pellets, bags for foodstuffs, tea bag wrapping pellets, and cigarette filters containing within the 3,479~15,770 chemicals per packing. The study utilizes ultra-high resolution electrospray ionization mass spectrometry, Fourier transform infrared spectroscopy, static and molecular dynamics quantum chemistry, and chemometrics.

Keywords: stochastic dynamics mass spectrometry, starch biopolymers, quantum chemistry, polylactic acid, 3D structural analysis

Received: June 15, 2024
Revised: August 3, 2024
Accepted: September 9, 2024
Published: September 11, 2024

Citation: Ivanova B. Structural Analysis of Polylactic Acid in Composite Starch Biopolymers – A Stochastic Dynamics Mass Spectrometric Approach. *Innov Discov*, 2024; 1(3): 26.

1 INTRODUCTION

Plastics are ubiquitous in the environment, due to their versatility, processing capabilities, low-cost, and barrier properties[1,2]. The synthetic polymers - long-chain organic molecules - are lightweight, durable, and pliable, among other properties; thus, making those attractive industrial materials over glass-, wood-, ceramics-, metal-, or paper-based ones for many applications. The durability and resistance of plastics to degradation processes in the environment cause end-of-life issues and; thus, the nature faces a significant threat, due to plastics-waste. There are research and technological disposal challenges, as well[2]. Circa 9500 million tons of plastics wastes have already been cumulatively over period 1950-2019. At about 5300 million tons of them had discarded as waste. There are only 600 million tons recycled plastics wastes. In parallel, there is expected grow of global production of plastics up to 1.2-1.3 billion tons by 2060[2]. Currently, only 9% of plastics waste has been recycled[3].

Solution of problems with environmental plastics waste, therefore, should multifaceted and accounts for entire life-cycle of polymers encompassing from production of plastics to its end-of-life governed by circular economy principles[4]. In the latter context, the so-called eco-friendly bioplastics play a crucial role in (partial) replacing synthetic plastics, particularly, underlying single-use materials such as food packaging[4-6], because of bioplastics are biodegradable compostable polymers and materials as well as they come from renewable

sources[7]. The eco-friendly bioplastics show lower carbon emissions, extra management possibilities of wastes over conventional plastics in order to decrease reliance on finite fossil resources, as well. Bioplastics minimize greenhouse gas emissions and exhibit improved functionality[8] as well as there is European standard EN13432, following a EU Directive on packaging and packaging waste (94/62/EC) determining compostable plastics as used to only packaging polymers[9,10].

The bioplastics can be metabolized by micro-organisms; thus, producing CO_2 and CH_4 as well as microbial biomass. Due to these reasons bioplastics do not accrue a footprint in the environment at their end-of-life[4]. Their end-of-life scenarios intended industrial composting, soil degradation, and anaerobic digestion, owing to the fact that the former approach is mainly used to compostable plastics waste.

Despite, the known degradation of bioplastics deteriorates into micro- and nano-plastics arises a question related to their effect on environment, as well as during their life time or before plastics complete degrade to CH_4, CO_2 and microbial biomass, because of there are statements that biodegradable micro- and nano-plastics have negative effect on plants and aquatic organisms. The latter concern is based on the fact that chemically, bioplastics are characterized by compositions of unstable ester bonds, which are susceptible to reaction of hydrolysis or enzymatic degradation in environmental conditions. There is consequent increasing in level of oligomers and monomers of biodegradable polymer components.

Due to reasons sketched above the United Nations Environment Programme has stressed that full substituting conventional plastics with biopolymers is not currently recommended. The latter is valid to conventional plastics, as well. The United Nations Environment Assembly meeting (2022) agree to establish a global Treaty, dealing with plastics pollution by 2024[11,12], but the alternative to replace completely conventional plastics with bioplastics has been scrutinized.

Despite, certified soil-bioplastics do not show ecotoxicity at concentration level of 1% w/w according to EN17033 standard determining concentration of ecotoxicity tests affecting on plant growth, microbial nitrification function, biomass, mortality, and reproduction of earthworms, respectively[4]. The concentration is at about two orders of magnitude higher than this one, which can be expected under field conditions[4]. There are concerns about plastics and bioplastics additives and their processes during degradable reactions, which could pose environmental threats, as well. The same is valid to presence of heavy metal ions in bioplastics; if any. There are scarce results from environmental sustainability of bioplastics; furthermore, data on environmentally relevant concentrations of wastes, their degradation products, and chemical components.

Therefore, bioplastics are an alternative replacing conventional plastics for industrial applications, including single-use plastic bags, agricultural mulch plastics, and more, however, remains the problem with their potential eco-toxicity as with the corresponding synthetic polymer composite materials.

In the latter context, utilization of polylactic acid (PLA) in replacing a lot of conventional plastics is mainly motivated by a lack of toxic composition, its glossy surface, efficient gas barrier characteristics commendable mechanical strength, optical transparency, and facile process ability[13]. PLA is eco-friendly, recyclable, energy-saving biopolymer[14] in addition to biocompatibility with human tissue[13].

PLA is obtained from fermentation of starch, sugar cane, and corn, together with starch-based polymers[7,15]. PLA, starch, dextran, and gelatin are used to fabricate 3D biomedical devices for tissue engineering. The PLA, amongst others polymers represents circa (ca.) 47% and 41% of total biopolymer consumption[7,16].

Further, advantage of PLAs is the fact that it used to textile sector and replaces synthetic polymers, as well. It emerges as prospective biopolymer, well-suited for industrial applications to many branches, ranging from agricultural and food technologies to medical applications and textile innovations. There are already developed PLA production schemes at an industrial scale. Currently, PLA and starch-based biopolymers production is ca. 60% of global bioplastics production[17]; furthermore, there is increasing in production to 1.8 million in 2025 tonnes[17]. European Bioplastics association have predicted that PLA shall be major market driver in the next years[14,16].

Food packaging is big market for plastics and production of new biopolymers is an absolute requirement for environmental, economic, and public health purposes[18]. Plastics packaging accounts for 30% of global plastics production. The food packaging industry has largest revenue of packaging plastics world-wide. In the latter context, PLA is a compelling alternative for food packaging, as well as, because of it has favorable mechanical and optical properties. As 100% bio-based plastics, it is currently being used in food-packaging industry[9] for vegetables, fruits, and biscuits films or containers, trays, yoghurt cups, fast food bowl, hot-food plate, etc[14].

Food packaging itself prevents foodstuffs from harmful chemicals, environmental pollution, pests, micro-organisms, and dust, respectively. It is utilized for protecting foodstuffs from physical damage, light, temperature, humidity, etc. also, it ensures easy transport to minimize food waste, or to protect food freshness. The food packing ensures supply chain from production to consumption[5,6].

Due to concern about possible migration of chemicals from food packing into foodstuffs; thus, causing for potential risk to human health and food, European Union Regulation Directive 1935/2004/EC established standards for packing materials coming into contact with foodstuffs, as well[19,20]. Thus, in highlighting PLA biopolymers as for food packaging materials, there should be underlined the aforementioned potential human health and eco-toxicity risk as its assessment, as well.

For the purposes of the current study, there should be also underlined bioplastics based on raw material used to PLA production. These are carbohydrate polymers such as starch, sugar cane, corn, and cellulose, respectively. They exhibit numerous advantages, as well. They are renewable or compostable materials; show easy tenable properties by mechanical adding of polyester resins; thus, modelling their mechanical properties, such as strength, flexibility, and thermal stability[21]. Due to these reasons, the demand has increased over recent years, especially for PLA and starch-based biopolymers as suitable candidates to replace plastics in food-packaging industrial sector[18].

Starch is used as a starting polymer for a large number of green materials[9]. In total, 75% of all organic material on the environment is in the form of carbohydrate (CB)-polymers. The starch and other carbohydrate(s) such as chitosan and cellulose or so-called bio-waste are big source of biodegradable polymers that can be utilized for diverse applications, including for food packaging industry[18]. Starch is promising biopolymer for industrial scale production of eco-friendly bioplastics, as well[22]. It consists of linear α-D-(l→4)- and branched via α-D-(1→6) glycoside bonds sub-units. However, hydrophilic OH-groups of chemically unmodified starch tend to form strong-to-moderate inter- and intramolecular hydrogen bonds; thus, limiting its application to many purposes[23].

Due to the latter reason, there is increased attention on chemically modified starch polymers, owing to the fact that oxidation reaction is one of the most important processes for chemical modification of biomacromolecules. It is broadly used to textile, paper, and more industrial sectors. The starch OH-groups at C^2-, C^3-, and C^6-positions, are modified to carboxyl and carbonyl-ones; thus, there is great challenge to improve mechanical and physico-chemical properties of starch[3,24], due to additional synthetic step of its chemical modification. It is transferred into thermoplastic derivative in presence of plasticizers such as glycerol, PLA, polyethylene, polyesters, sorbitol, water, poly(butylene succinate), etc. Both PLA and CB polymers are principal component of prospective biopolymers capable of replacing conventional food-packing polymers.

Further, there is also used, natural polymers such as cellulose as aforementioned. It has a broad spectrum of applications to many industrial branches and is used to paper products, biofuels production, textile fibres, and platform chemicals, etc[25]. Particularly, this study analyses few cellulose-based tea bag and chocolate wrapping samples, among other, as well. Cellulose is one of the most prominent bio-reinforcements for PLA, despite the fact that like starch, it does not change significantly the molecular structure, mechanistic characteristics, physico-chemical properties. It is difficult an industrial scale competition for marked production of cellulose based food packing materials comparing with those of synthetic polymers. Despite, the significant importance of cellulose oligosaccharides to many industrial braches there is a rather lack of their systematic research, mainly, due to its limited availability and high price, but starch- and cellulose-based bioplastics show stronger mechanical properties comparing with other biodegradable materials, including synthetic polymers such as poly(methyl methacrylate).

Due to the latter reason enormous research effort is shifted into direction of chemically substituted CBs derivatives[3], which are very prospective research strategy for elaboration and development of new CBs-based functional bioplastics biodegradable or compostable ones, or both of these under industrial manufacturing conditions; furthermore, coming from renewable resources. Also, both the cellulose and starch are most relevant dietary biopolymers[26,27]. Compared to PLA, cellulose, and starch exhibit higher safety and edibility[15]. They can be found in all living systems[26] and play important role in biological processes[28]; furthermore, there should be highlighted the natural availability of CBs such as cellulose, as well. The biomass, in the latter context, is the most abundant source of carbon in the environment. It is mainly composed by CBs. In addition, it is prospective low-cost feedstock for purposes of the chemical industry.

The biomass is environmentally friendly, renewable, and carbon-negative source[29], also trapping and using CO_2 for purposes of photosynthesis. It is promising sources of energy, as well. The use of lignocellulose biomass, such as agricultural by-products, is considered to be a green approach to produce biofuels and biochemical[30]. A reason governing interest in PLA production also aims at reducing societies' dependence on fossil resources. The Russian Federation have established priorities until 2035 in the sphere of renewable sources of energy using biomass[31], including commercial production of biomass; thus, resources could be used for both biofuel production, despite, high supply of high-value fossil fuels, respectively, bioplastics production, or be exported.

Therefore, both environmental problems, due to

food packing synthetic plastics wastes and energy have become major problems of survival and development of the current human society, amongst others, and the biomass processing as well as (partial) replacement of synthetic polymers with CBs-composite biopolymers of many industrial applications could alternatively solves many of these problems[32].

However, since bioplastics cannot completely degrade in natural or industrial settings[33] as the corresponding conventional polymers, which are complex mixture of known and unknown chemicals encompassing (bio) polymers, fillers, plasticizers, stabilisers, pigments, flame retardant, antioxidants, and more, as sketched above[33,34], there is an affect on affinity of bioplastics toward sorption reactions of metal ions from particular aquatic environmental water[35,36], as well. The latter processes are governed mainly due to increased oxygen-containing groups on the surface of the discussed CBs based biopolymers.

Furthermore, there are concerns not only with the latter issue of environmental protection from bioplastics waste due to competitive reactions of sorption of organics and heavy metal ion containing inorganics, but also with reactions of polymerisation of food packing materials; if any, which can produce inclusions of oligomers into the bulk biopolymer which are considered as no intentionally added chemicals[24]. Oligomers could migrate from polymer packing to foodstuff; thus, compromising the safety for the consumers. The same is true for a large number of additives to polymers[35]. Such low-molecular-weight (LMW) can be released at all stages of lifecycle of both synthetic and biodegradable polymers via processes of migration or via volatilisation.

Therefore, transfer of chemicals from polymer packages to foods, human, and the environment occurs. Due to these reasons pure biopolymers are regulated via Directive of European Union (1935/2004/CEE), while additives are regulated via Directive of European Plastics Regulation (10/2011)[37]. The maximum allowed migration concentration limits for chemicals which are not explicitly listed in the latter Directive must be lower than 0.01mg/kg food stimulant or foodstuff.

Analytical determining of the latter chemicals should be compulsory done within the framework of established legislation Directives and protocols should be agreed with Council Directive 96/23/EC concerning performance of analytical methods and techniques as well as interpretation of results, particularly, focusing the reader attention on requirements for mass spectrometry (MS) and infrared (IR)-spectroscopic approaches[38].

In addition, it should be stress, that currently evaluation of polymers sustainability often disregarded affect on human exposure to chemicals[33]; thus, assessing potential toxicity of new biopolymers, as well. Derivatives of cellulose-based polymers, which are already widely used to many industrial branches; thus, manufacturing thickener, dispersant, adhesive, emulsifier, petrochemical products, filler, ceramics, synthetic resins, textiles, synthetic resins, foods, pharmaceutics and components in oral medications due to their lack of toxicity[39] show a rather lack of data on their chemical safety; thus, making a problematic gap in knowledge, due to increased application to bioplastics. Many conventional polymers contain toxic *in vitro* chemicals[33,34], as well. However, the same is true for bioplastics[35]. Analytes of both the synthetic and biopolymers can be toxic[33].

Hence, I am undertaken to describe links among bioplastics, their ecotoxycological affect, sketched in preceding paragraphs, food packing, and crucial innovation and prospective application of stochastic dynamics mass spectrometric method presented in this study both to fundamental research and industry. It, in fact, establishes relation among them, due to following reasons.

There could be said that there is crucial innovative relation between environmental protection from potential toxicological effect of bioplastics; biodegradable food packing made by bioplastics, and assessment of risk for human health together with the risk for environment, and stochastic dynamics mass spectrometry as still the title of the study implies.

The structural analysis of intermediates of interaction of components of biomass is crucial in revealing mechanistic aspects of chemical reactivity of CBs. The CBs ring cleavage mainly results to linear molecules or cyclization reaction products. The molecular structural determining of interacting derivatives is significantly complicated, due to diversity of molecular structures and glycoside linkage types as well as series of intramolecular rearrangement processes of the major constituents, themselves.

On the other hand, the first step in studying biological functions of CBs is their structural determination that involves identification saccharide components, determination of monomer sequences, and 3D structural analysis, as well.

One might conclude from the sketched above complexity of biopolymer composite materials that it is not possible to establish the 3D molecular structures of their components.

Perhaps, one should confine her, respectively, his attention to develop innovative stochastic dynamics MS method as an effort to establish an unified standard highly accurate-to-exact analytical quantitative and structural

procedures applicable to analyse the same object in composite biopolymers and their derivatives based on CBs and PLA, because of MS methods have ultra-high accuracy and sensitivity; tolerated determining of complex mixtures of analyses at very low levels of concentrations, and appear a natural choice for analysis of this class of molecules, i.e., carbohydrates[40].

In particular, the irreplaceable capability of mass spectrometry as robust analytical approach to analyse structurally CBs has been illustrated persuasively looking at its use to understand of the ubiquitous role of CBs in the glycobiology. Mass spectrometry creates innovative demands for analytical approach to structure elucidation of oligosaccharide compositions, their branching and sequences, type of glycoside linkage, anomericity and ring sizes and absolute configuration, respectively.

Despite, compared to advances of mass spectrometry in proteomics[41] progress in its application to CBs has evolved slowly, due to the fact that CBs are significantly more challenging set of molecular targets for 3D structural analysis, due to reasons sketched above. Furthermore, biosynthesis of CBs is not template-driven process and the discussed biopolymers can be found in the nature as heterogeneous material. The CBs heterogeneity affects on metabolic fate, biological activity, solubility, and stability, respectively.

The cellulose decomposition itself in water yields to glucose, xylose, mannose, fructose, and degradation products of cellulose, in addition to unidentified constituents[25]. As minor degradation products of oligosaccharides of cellulose are shown levoglucosan, fructose, xylose, xylose, erythrose, dihydroxyacetone, glycol aldehyde, glycolic acid, lactic acid, pyruvic acid, glycerol acid, 2,4-dihydroxybutanoic, erythronic acid, gluconic acid, 5-hydroxymethylfurfural, reductic acid, catechol, pyrogallol, among other miscellaneous and sugar-type compounds.

Despite, that molecular structural analysis is the primary research task of analysis of a CBs polymer and there are several mass spectrometric methods as well as other analytical methods and techniques which are fruitfully used for polymers structural determination it does not represent trivial research task. Rather, it is significantly challenging research effort because of 3D molecular structural analysis of polymers proves not only successful polymer synthesis, but also identify and annotate unexpected side-chain products of polymer reaction products, including trace analyte amounts of polymer inclusions, having, however, critical health-related implications[32]. The application of MS methods to polymer research is the same to this one in omics-methods of biology and medicine[42]. Mass spectrometry has been widely used in structural elucidation of oligosaccharides due to its high accuracy, analytical versatility and high sensitivity, but, due to significant complexity of the composite polymers there are highlighted limitations to a broad application of MS methods to polymeromics.

Thus, (1) the polymer must be capable of stabilising gas-phase ions; (2) in cases of highly complex mixtures of polymers containing unknown oligomers and monomer derivatives as food-packing samples studied, herein, often, conventional MS techniques for data processing of measurable variables do not provide specific data on functional groups of polymers or on analyte primary and higher-order molecular structure; and (3) polymeric mixtures could not be determined properly, due to different ionisation or detection efficiencies of the constituents of the polymer.

The soft-ionisation MS methods; for instance, matrix-assisted laser desorption/ionisation, electrospray ionisation, and atmospheric pressure chemical ionisation ones have pioneered the field of polymeromics[43]. The same tools are broadly used to analyse biologically active macromolecules such as peptides, proteins, and lipids, together with CBs are shown, above. The tandem MS/MS operation mode in polymer research is mainly applied to: (1) identify and annotate organic additives in polymers, owing to the fact that the additives are LMWs; (2) determine volatile polymer pyrolyzates; and (3) determine individual oligomers in LMW polymers. The MS m/z data on n-mers of polymers are used to obtain molecular weight of analyte, its compositional heterogeneity, and analyte functionality distributions.

Since, a composite polymer can be complex chemical mixtures having isobaric analyes or it can be mixture of isomeric 3D structural architectures of analytes, then, it can be even impossible to determine polymers or oligomers in mixtures by single-stage MS measurements of m/z data alone and conventional MS methods for data processing of measurable variables. Thus, MS methods mainly use tandem operation mode, however, its often enables compositional identification of carbohydrates; thus there is a, rather lack of universal and single method for structural characterisation of CBs.

In the latter context, nuclear magnetic resonance spectroscopy is robust approach to characterise polymers; thus, determining repeated molecular monomer structural unit of polymers and their end-chain groups. The method shows low sensitivity and challenging data-processing tasks, due to effects of peak broadening, time of analysis, and chemical shifts[43]. Nuclear magnetic resonance spectroscopy is used to elucidate structurally polymers; however, it requires rather pure samples and shows a lack of capability of revealing polymer sequence data. X-ray diffraction is also robust analytical approach to determine 3D structure and morphology of 0.3-0.5 and 1-200nm scale

samples of polymers. It determines oligomer or polymer shapes and self-organisations of polymer chains, but the typical weak scattering intensities can limit application of the method to polymer structural analysis. Thermal approaches such as differential scanning calorimetric and thermogravimetry find application to polymer research, as well. There are determined glass transition temperature of materials, their crystallisation and melting temperatures[43]. Various infrared and Raman spectroscopic methods are also applied to study (bio) polymers in plants or quality parameters in horticultural and agricultural crops. The vibration data on can be obtained directly on plant tissues or on isolated fractions of plant material by hydrodistillation or solvent extraction. Application of FTIR spectroscopy to study plastics is known.

The current study shall demonstrate how sketched in the introductory section problems of mass spectrometric analysis of mixtures of polymers can be bypassed by application of the innovative stochastic dynamics mass spectrometric model Equations (2), and (4) to determine exactly 3D molecular structures of composite carbohydrate mixtures of biopolymers of commercial food-packing of bio based biodegradable single-use drinking cups, films and pellets of PLA of fermented corn starch, plant based bag for foodstuffs, tea bag wrapping pellets, and cigarette filters of wood cellulose as well as potato and corn starch containing within the 3,479~15,770 chemicals per biopolymer sample. The method focuses on methodological innovations of the analytical mass spectrometry as irreplaceable approach to quantify and determine 3D molecular structural analytes in complex industrial scale implemented commercial biopolymers. It contributes crucially not only to development of green food-packing technology and to create a sustainable, carbon neutral society, but also to solve problems of environmental pollution of food packing plastics. The major goal of the study includes further developing and establishing of the innovative analytical mass spectrometric approach to both the analytical chemical fundamental science and industry; thus, solving and capturing problems find in applying conventional methods and technologies for the analytical mass spectrometry in studying biopolymers. Thus, we aim to replace routine analytical methods with innovative stochastic dynamics approach. Despite the fact, there is scarce application of the new mass spectrometric approach, so far, which makes the latter statement a bold one and hot topic, however, we are mainly headed towards that direction.

2 EXPERIMENTAL

2.1 Materials, Methods, and Samples

The study uses experimental data on Fourier transform infrared (spectroscopy) and mass spectra of cellulose, starch, and PLA samples of commercial bioplastics[33]. The experimental raw files are public available and can be downloaded free of charge[44]. There are used the following mass spectrometric raw files: PLA_01.raw, PLA_06.raw, Starch_1.raw, Starch_3.raw, Starch_5.raw, Starch_6.raw, and Starch_7.raw, Cellolose_1.raw, Cellulose_2.raw, Cellulose_3.raw, Celluose_4.raw, and Cellulose_6.raw, respectively. The sample description is shown in Table 1 and Table S1. The sample preparation tasks have been described[33,44]. Importantly, extracts may contain nano- and microplastics.

Solid-state infrared spectra of film samples within mid-region of the electromagnetic spectrum have been measured on FTIR Perkin Elmer Spectrometer (Waltham, Massachusetts). There is used conventional (KBr pellet) and linearly polarised spectra were recorded within the range 4,000-400cm^{-1} on a Bomem-Michelson 100 FTIR-spectrometer (Bomem Inc., Canada) equipped with a Perkin Elmer wire-grid polarizer. The IR-spectra of standard samples were recorded on a resolution of ± 1cm^{-1} and 150 scans per spectrum. The spectra were recorded, using Nd:YAG laser (l_{max}=1024nm). The scan speed of the used moving mirror was 0.5cm·s^{-1}. Standard sample of CBs were used (Sigma Aldrich Inc.)

Ultra-high performance liquid chromatography coupled to quadruple time-of-flight mass spectrometry/mass spectrometry has been used: Acquity UPLC Waters Liquid Chromatography system and SYNAPT G2-S mass spectrometer (Waters Norge, Oslo, Norway), operating in positive polarity. Two µL CH_3OH extracts (0.15mg plastic µL^{-1}) have been injected onto a Waters C18 guard column coupled to an Acquity UPLC BEH C18 column (130Å, 1.7m, 2.1×150mm, Waters) with a column temperature of T=40°C. The LC flow rate has been 0.2mL·min^{-1} using H_2O with 0.1% HCOOH and CH_3OH with 0.1% HCOOH as mobile phases A and B. Detail on the experimental design can be found[44].

2.2 Theory/Computations

2.2.1 Stochastic Dynamics Mass Spectrometry

Stochastic dynamics uses Equations (1) and (2); thus, underlying them methodologically in the mass spectrometry. The goal is not to show their complete set of devising steps, but rather, to highlight the novelty to field of analytical mass spectrometry and those advantages that are in particular prominent in debates emerging from method performances of conventional MS tools for data-processing of CBs measurands and applicability of MS methods to determine exactly 3D molecular structure of such analytes. The Equation (2) prospective alternative tool for quantitative and structural MS based analyses of complex CB-mixtures of commercial composite polymers, including food packing.

Thus, MS mensurable data i.e., mass-to-charge and intensity values of ions of analytes are described as random variables; thus, assuming that mass spectrum

Table 1. Plant-based Polymer Products According to Work[44]

Sample/ Plastic Type	Plastic Product	Colour, Printing Ink	Material Information from Producer/Distributor/Vendor
Starch_1	Disposable cutlery	Beige	60% starch, 40% PP, for cold and hot foodstuff, temperature tolerance up to 104°C
Starch_3	Film	Beige	100% corn-stach
Starch_5	Pellet	Beige	Plasticizer-free, contains natural potato-starch and other biologically sourced polymers, suitable for fruit and vegetable bags, fully biodegradable and compostable according to EN 13432
Starch_6	Pellet	Beige	Biobased or plant-based content of > 60%, biodegradable, application also consumer good, packaging, food sector
Starch_7	Waste bag	Transparently green	Starch blend, made of Mater-Bi®, compostable, biodegradable
PLA_01	Single-use drinking cup	Transparent	Fermented corn-starch, pure PLA, renewable material, compostable.
PLA_10	Pellet	Transparent	PLA homopolymer, compliant with food contact regulation EU 10/201, in compliance with the EN13432 and are certified compostable by Vincotte and by European Bioplastics

can be reliably described and predicted *via* tools generating random numbers. There is used modified Box-Müller approach for generating random numbers using its basic Equation (S1)[45]. Equation (S2) is derived from Equation (S1). The *x* and <x> denote stochastic variable and its average value. The P_1 and P_2 are random number, while σ^2 denotes variance. It is given by Equation (S3). The intensity of MS peak is described as random variable and *x*=I. It has been proven that $\ln P_1 = -17.0533_{(7)}$ for all MS measurable variable intensity (I) of MS peaks over any span of scan time under many ionisation methods used to measure mass spectrum of analytes[46-49]. The Equation (S4) applid to data on temporal distribution of PLA product ions at m/z 433.13867 and 217.07353 again confirm the validity of the statements written in this sub-section (see sub-section 3.3.1. Calculation of stochastic dynamics parameters, below, and data on Table S5.

Further: There is relation $A=-2\sigma'^2.\ln P_1$ having not only statistical significance, but rather physical meaning. The parameters σ^2 and $\sigma^{2'}$ are independent of each other. It is used Ornstein-Uhlenbeck's approximation ($\sigma^{2'}=2\beta^2.D$) to σ^2 and Einstein's one to parameter $\beta=3.10^{-8}$ and Equation (S4) is given by Equation (S5).

The substitution of these relations yields to Equation (1). It is exact model connecting between diffusion parameter and experimental MS intensity written as $(I-\langle I\rangle)^2$. The statistical parameter 'A' is obtained *via* SineSqr curve fitting of experimental relation $(I-\langle I\rangle)^2=f(t)$ where t denote time. Thus, parameter 'A' accounts for temporal distribution of intensity (I) of MS peak of analyte ion over any random span of scan time of measurements.

$$D_{SD}^{tot} = \sum_i^n D_{SD}^i = \sum_i^n 1.3194.10^{-17} \times A^i \times \frac{\overline{I_i^2} - (\overline{I_i})^2}{(I_i - \overline{I_i})^2} \quad (1)$$

However, depending on complexity of function $(I-\langle I\rangle)^2=f(t)$ or temporal behavior of measurand intensity over a studied span of scan time, there can be expected deviations from absolute correlation ($|r|=1$) of SineSqr curve fitting procedure[47]. For instance, consider detail on temporal distribution of PLA product ions at m/z 433.13867 and 217.07353 (Figure S1).

In solving the latter problem, Equation (1) there is simplified, using approximation that $A \equiv 2.\langle (I-\langle I\rangle)^2\rangle$; thus, writing Equation (2). It is capable of exact quantifying analytes and determining 3D molecular structure of analyte on the base on MS soft-ionization methods.

$$D_{SD}^{'',tot} = \sum_i^n D_{SD}^{'',i} = \sum_i^n 2.6388.10^{-17} \times \left(\overline{I_i^2} - (\overline{I_i})^2\right) \quad (2)$$

$$D_{QC} = \frac{\prod_{i=1}^{3N} V_i^0}{\prod_{i=1}^{3N-1} V_i^s} \times e^{-\frac{\Delta H^{\#}}{R \times T}} \quad (3)$$

The exact 3D structural analysis *via* Equation (2) is carried out complementary with Arrhenius's Equation (3). The assignment of MS peaks of analyte is performed *via* chemometrics assessment of relation $D''_{SD}=f(D_{QC})$ of parameters of Equations (2) and (3) owing to the fact that relation $D''_{SD}=f(D_{QC})$ shows $|r|=0.9999_4$, studying data on LMW analytes. It has been found that D_{QC} parameter accounts precisely for energy parameters of 3D molecular structure and isotopologies of analyte molecule, as well[46].

Equation (3) has been further modified (2023) yielding to Equation (4)[48]. It appears reliable tool for predicting MS spectra of analytes.

$$I_{SD}^{Theor} \sim \left(2.6388.10^{-17} \times D_{QC}\right)^{1/2} \quad (4)$$

Equation (4) uses approximations $\langle I^2\rangle > \langle I\rangle^2$ and $D''_{SD} \sim D_{QC}$, where I_{SD}^{Theor} shows intensity value peak of

q^{th} product ion obtained depending on experimental conditions of MS measurements.

Scarce applications, so far, of Equation (4) yield to $|r|=0.9992_2$-0.99; thus, correlating between theory and experiment or between I_{SD}^{Theor} and I_{av}^{TOT} data on analytes. There have been studied plant metabolites and oligopeptides[48]. Its reliability to determine synthetic polymer has shown $|r|=0.9999_8$[49].

2.2.2 Computational Quantum Chemistry

GAUSSIAN 98, 09; Dalton2011 and Gamess-US program packages were used. Ab initio and DFT molecular optimisation were performed by B3PW91 and ωB97X-D methods. The Truhlar's functional M06-2X was utilized. The algorithm by Bernys determines ground state (GSs). PES' stationary points were obtained by means of harmonic vibration analysis. Minima of energy are confirmed when there is a lack of imaginary frequencies of second-derivative matrix. Basis set cc-pVDZ by Dunning, 6-31++G(2d, 2p) and quasirelativistic effective core pseudo potentials from *Stuttgart-Dresden(-Bonn) (SDD, SDDAll, (*http://www.cup.uni-muenchen.de/oc/zipse/los-alamos-national-laboratory-lanl-ecps.html*) were utilized.* The ZPE and vibration contributions have been accounted for up to a magnitude value of 0.3eV. Species in solution were studied by explicit super molecule and mixed approach of micro hydration by PCM. The ionic strengths in solution were accounted for, using IEF-PCM. Merz-Kollman atomic radii and heavy atoms UFF topological models were used. The pH effect was evaluated computing properties in neutral and cationic forms. Molecular dynamics (MD) computations were performed by ab initio Born-Oppenheimer molecular dynamics (BOMD) was carried out at M062X functional and SDD or cc-pvDZ basis sets, as well as, without to consider periodic boundary condition. The trajectories were integrated using Hessian-based predictor-corrector approach with Hessian updating for each step on BO-PES. The step sizes were 0.3 and 0.25amu$^{1/2}$Bohr. The trajectory analysis stops when: (a) Centres of mass of a dissociating fragment are different at 15Bohr, or (b) when number of steps exceed given to as input parameter maximal number of points. The total energy was conserved during computations at least 0.1kcal·mol^{-1}. The computations were performed *via* fixed trajectory time speed (t=0.025fs) starting from initial velocities. The velocity Verlet and Bulirsch-Stoer integration approaches was used.

The Allinger's MM2 force field was utilized[50]. The low order torsion terms are accounted for higher priority rather than van der Waals interactions. The method's accuracy is 1.5kJ·mol^{-1} of diamante or 5.71.10^{-4}a.u.

2.3 Chemometrics

Software R4Cal Open Office STATISTICs for Windows 7 was used. Statistical significance was evaluated by t-test. Model fit was determined upon by F-test. Analysis of variance (chemometric method) (ANOVA) tests were used. The nonlinear fitting of MS data was performed by means of searching Levenberg-Marquardt algorithm[51]. Together with ANOVA test, there are used nonparametric two sample Kolmogorov-Smirnov, Wilcoxon-Mann-Whitney, and Mood's median tests, as well. ProteoWizard 3.0.11565.0 (2017), mMass 5.0.0, Xcalibur 2.0.7 (Thermo Fischer Scientific Inc.) and AMDIS 2.71 (2012) software were used. The FTIR-spectrometric patterns were processed by means of GRAMS AI 7.0 software (Thermo Fischer Scientific Inc.)

3 RESULTS AND DISCUSSION

3.1 Fourier Transform Infrared Spectroscopic Data

If we shift in this sub-section to focus on experimental vibration characteristic modes of starch- and PLA-based samples, then correlation between molecular structure of components of bulk polymers lies in functional relation between common characteristic IR-modes; if any. In detailing on the latter issue there are shown Fourier transform infrared (FT-IR) spectra of PLA-samples (Figure S2). They are characterized by significant similarity; thus, excluding from samples PLA_05 and PLA_06. PLA-samples reveal typical for PLA IR-bands of C=O stretching vibration ($\nu_{C=O}$) within 1750-1700cm^{-1} and $\nu^{as}_{C\text{-}O\text{-}C}$ and $\nu^{s}_{C\text{-}O\text{-}C}$ stretching vibrations at about 1,110 and 950cm^{-1}[52]. The IR-bands at 1,150 and 950cm^{-1} are assigned to $\nu^{as}_{C\text{-}O\text{-}C}$ and $\nu^{s}_{C\text{-}O\text{-}C}$ stretching vibrations of monomeric structural units of cellulose, as well as, while the low-frequency shifting of $\nu_{C=O}$ band of PLA_05 and PLA_06 biopolymers can be associated with cyclic lactose. It should be accounted for the fact that the wood cellulose also reveals $\nu_{C=O}$ band at 1,717cm^{-1}, however. The same is valid to oxidised products of cellulose showing IR-band at 1724cm^{-1} of $\nu_{C=O}$ stretching vibration of COOH-group[53].

Due to reasons highlighted above the observed overlapped regions of IR-vibrations of PLA and cellulose prevents from an unambiguous FT-IR-based structural assignment of components of composite biopolymers based on PLA, starch, and cellulose. Some results are illustrated as Figure S3 and Figure S4 and data on Table 2 and the reader interested in application of the method to determine analytes in PLA and starch-based biopolymers should detail on, as well. There is significant similarity of IR-patterns of sample PLA_01 and Starch_6; thus, assuming presence of the same major component of the biopolymers.

Similar characteristic IR-bands can be found in Cell_3 sample of cigarette filter of unbleached cellulose and standard sample of sucrose and Starch_3 sample of 100% corn starch, as well (Figures S4-S6) The IR-spectroscopic region of monomers and polymers of CBs is characteristic of molecular conformation toward (C)O-C^{6}H$_2$-structural-unit. Comprehensively, relations between 3D structure

Table 2. Characteristic IR-bands of Plant-based Polymer Products

Sample	Wavenumber (cm^{-1})/Assignment				
	$\nu_{C=O}$	ν_{C-O} (COOH)	ν^{as}_{C-O-C}	ν^{s}_{C-O-C}	$\nu_{(CO)C-C}+\gamma_{(CO)C-C}$
PLA_01	1,749.01±0.4	1,259.58±1.03	1,182.94±4.1	954.45±1.33	875.11±0.0
	-	-	-	-	754.15±0.8
	1,759.76±1.0	1,271.66±4.22	1,189.71±1.2	935.28±0.66	-
PLA_06	1,729.24±0.1	-	-	-	-
	1,713.55±2.2	-	-	-	-
Starch_3	1,720.35±0.2	1,277.45±1.11	1,094.08±1.1	941.75±0.34	727.87±0.2
Starch_5	1,707.67±2.0	1,268.98±0.05	1,106.78±2.2	-	868.40±0.1
	1,745.44±4.0	1,249.71±3.13	1,182.95±3.1	935.17±4.13	878.27±1.3
Starch_6	1,715.23±7.8	-	-	-	756.44±3.1
	-	-	-	-	725.47±0.1

and position of stretching and bending modes of discussed functional group have been studied[54]. In the case of Starch_6 sample to the discussed IR-mode, there is assigned band at 878.27cm^{-1}, while PLA_01 sample shows IR-mode at 878.11cm^{-1}. An IR-band at about 750cm^{-1} cans be found in the two samples, as well. The IR-spectroscopic region within 950-850cm^{-1} is widely used to analytical purposes[55,56], particularly, distinguishing between mono- and CBs disaccharides. IR-band at 874cm^{-1} is assigned to D-glucose (Gly). It can be found in IR-spectrum of cellobiose, as well. The vibration mode is assigned to bending vibrations of OC^6H and C^5C^6H groups. To the latter mode there are contribution to stretching vibrations of C^5-O and C^5-C^6 bonds, as well. The data on CBs samples studied, herein, agree well with FT-IR spectroscopic results from various standard CBs, starch and cellulose based biopolymers.

The IR-patterns of PLA-samples reveal strong intense IR-band at 728cm^{-1} (PLA_06.) It is assigned to bending vibrations of CCO groups in addition to CCC and COC groups of pyranose ring of CBs. Owing to the fact that sample PLA_06 shows a low frequency shifting of $\nu_{C=O}$ mode and, in parallel an intensive band at 728cm^{-1}, there can be assumed that it contains cyclic lactide, rather than linear PLA oligomers (Figure S3). Importantly, synthetic polymer poly (ethylene glycol) is characterised by IR-band at 721cm^{-1}. Thus, there can be proposed, looking at IR-pattern of PLA_06 a presence of component based on synthetic modified polyethylene glycol, as well. The statement agrees well with experimental data on PLA_06 (retention time (RT)=4.74-4.80) mins showing ions, having spaced between peaks Δ(m/z)=14 (Figure S7) It is characteristic value of poly (ethylenglycol)methylether.

3.2 Mass Spectrometric Data

3.2.1 Mass Spectrometric Data on Cellulose- and Starch-based Bioplastics

Starch 3, Starch 5, and Cell_3 samples show typical for cellulose and starch product ions (Figures 1, 2 and Figures S8-S10). MS peaks at m/z 1073.35, 911.29, 749.23, 587.18, 425.12, and 263.06; 1157.38, 995.32, 833.22, 671.21, 599.16, and 347.10, as well as 689.23, 527.17, and 365.11 have spacing of Δ(m/z)=162. Figures S11-S13 depict chemical diagrams of CBs ions depending on isomers and protomers. Common MS peaks of both the cellulose and starch have been assigned to sodium adducts of CB-dimers and oligomers as well as ions of loss of solvent water molecule[57,58]. Correlative analysis between intensity data on peaks at m/z 365.11383, 527.16528, and 689.22754 of Cell_3 and Starch_5 having virtually identical m/z measurands shows |r|=0.8406. The parameter highlights clearly the major line of reasoning described in this study sketching an account of crucial role of developing of methods for exact data-processing of MS intensity parameter. As discussed, results show m/z parameters of product ions of both the cellulose and starch are virtually identical. Thus, common species of fragmentation of the polymers can be distinguished reliably only evaluating exactly intensity data on the MS peaks of their ions.

The corresponding MS peaks of observable species at m/z 973.34, 811.29, 649.23 487.18, and 325.12 of Starch 3 are assigned to oxonium type CB dimers and oligomers. As can be expected, they also show MS peak spacing Δ(m/z) =162. In the latter context, if we describe observed product ions from perspective of common scheme of [L], [R], and [M] type oligomers, then in both the samples Cell_3 and Starch_3, there can be found common [R] and [M] type CB-dimers and oligomers as well as their alkali metal ion adducts. The same is true for Starch_5 containing potato-starch. The MS peak spacing of CBs oligomers and polymers are often associated with loss of monomeric anhydrous-saccharide sub-unit (162Da). The theoretical structural analysis of MS ions accounts for CBs isomerism and frequently occurring positional isomers looking at α-1,4- and α-1,6-connectivity as well as α-1,4- and β-1,4-configurations[59].

However, MS/MS spectrum of maltohexaose $[M+H]^+$ cation reveals peaks at m/z 991.338, 973 ($[M-H_2O+H]^+$), 811.272, 649.212, 487.166, 325.113, and 163.062 having spacing Δ(m/z)=162[60]. They are analogous

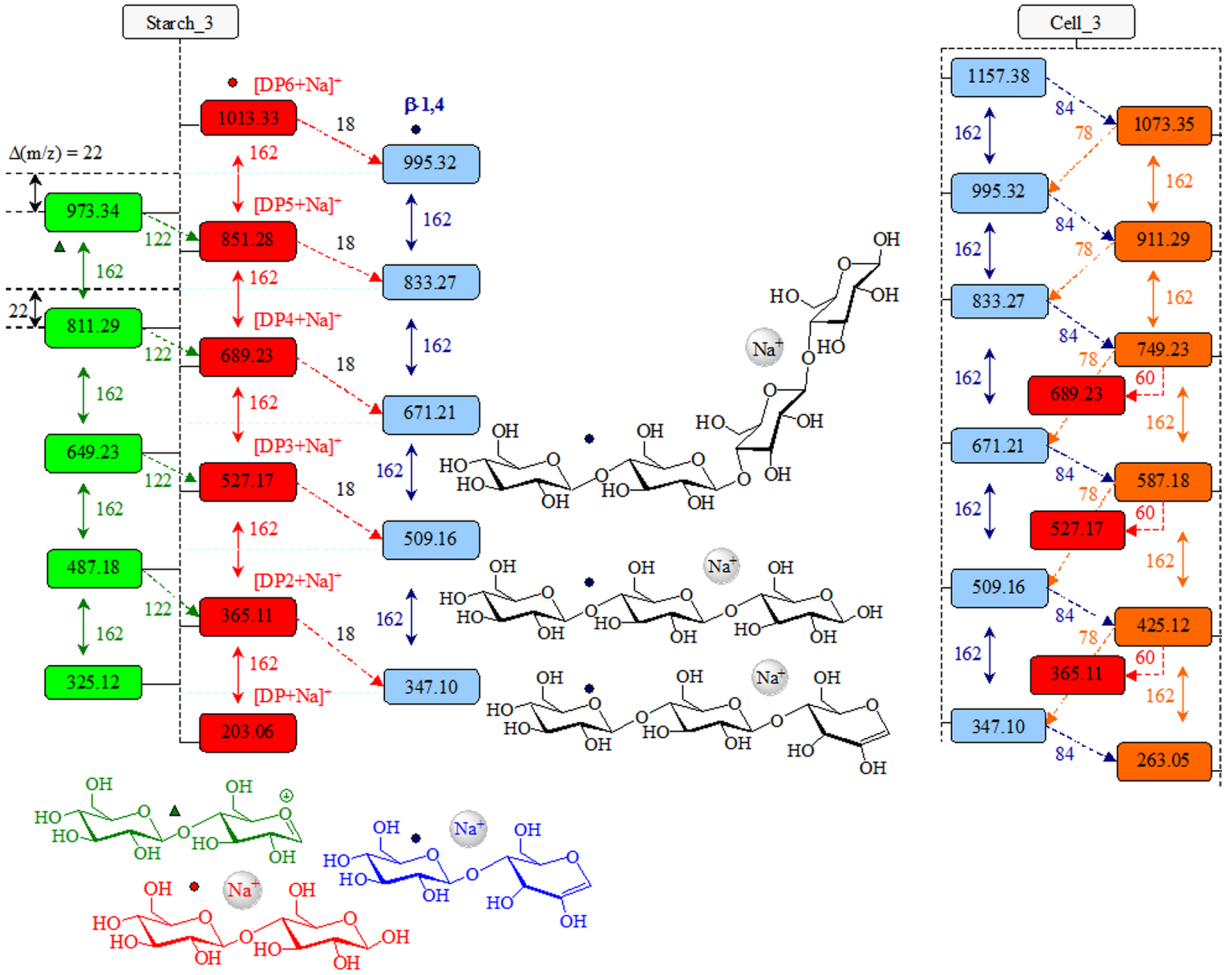

Figure 1. Mass spectrometric data on carbohydrate parent and product ions of Starch_3 and Cell_3 biopolymers; chemical diagrams of observable ions.

of MS pattern of Starch_3. The latter fact complicates significantly the assignment of species of CBs in starch samples; furthermore, owing to the fact that dextran - a polysaccharide, derived from lactic acid bacteria - shows peaks at m/z 1013.3145, 851.2630, 689.2103, 527.1568, and 365.1024 assigned to sodium adducts of CB-oligomer $[M_n+Na]^+$, where n=6-2. As can be seen they are identical with data on Strach_3 and dextran.

MS peaks of dextran are assigned[32] to: m/z 1,013.3604, 851.2573 (Y_5), 833.2396 (B_5), 689.1794 (Y_4), 671.1621 (B_4), 527.1093 (Y_3), 365.1093 (Y_2), 347.1051 (B_2), 331.1155 ($B_2/^{0,5}A_2$), 317.0911 ($B_2/^{0,1}A_2$), 305.0989 ($^{0,2}A_2$), 245.0847 ($^{0,4}A_2$), and 222.4961 ($^{1,5}X_2$,) respectively. It shows α(1→6) glycoside linkage; thus, comparing data on β-(1→4) and α-(1→6) linkage in MS spectrum of Starch_3 within RT =1.68-3.24min. The detailed fragment pattern uses the nomenclature by Dommon and Costello[61]. Typically, MS peaks of isotopomers of α(1→6) glycoside bonded CBs have been studied[62]. (Consider MS molecular isotopologies[40,46]).

Moreover, complication of exact assignment of MS peaks in Strarch_3 within scan numbers 155-399 follows from identical product ions of maltopentaose and 3α,6α-mannopentaose. The analytes show peaks at m/z 851, 833, 671, 487, 352, and 163 of sodium adducts, while in CID-MS/MS conditions there are peaks at m/z 811, 649, 487, 325, and 163, respectively. These are the same m/z values of sample Starch_3. The 3α,6α-mannopentaose is branched CBs.

Thus, there is performed a comparative analysis of data on Starch_3 and standard samples of analyte examining statistically intensity data on shown their characteristic peaks. The linear relation between intensity data on MS peaks of maltopentaose and 3α,6α-mannopentaose yields to |r|=0.78303 (Figure S14). There is |r|=0.98 in assessing data on peaks of the same analytes in CID-MS/MS conditions of measurements. Correlation between intensity data on maltopentaose and 3α,6α-mannopentaose with CBs species in Starch_3 within 180-300 scan numbers and peaks at m/z 163.06538 (I=22,046.973arb.units), 325.11935 (60571.499), 487.1806 (9,950.825), 649.23102 (4,781.8515), 671.20953 (11,444.525), 811.28546 (2,007.978), 833.27344 (3,479.052), and 851.2843 (12,101.471) yields to |r|=0.1785 and |r|=0.27865 (maltopentaose), and |r|=0.0716 (3α,6α-mannopentaose.) The latter result assumes that there is unable to assign with a high statistical significance CBs of Starch_3 sample neither to maltopentaose, nor to 3α,6α-mannopentaose;

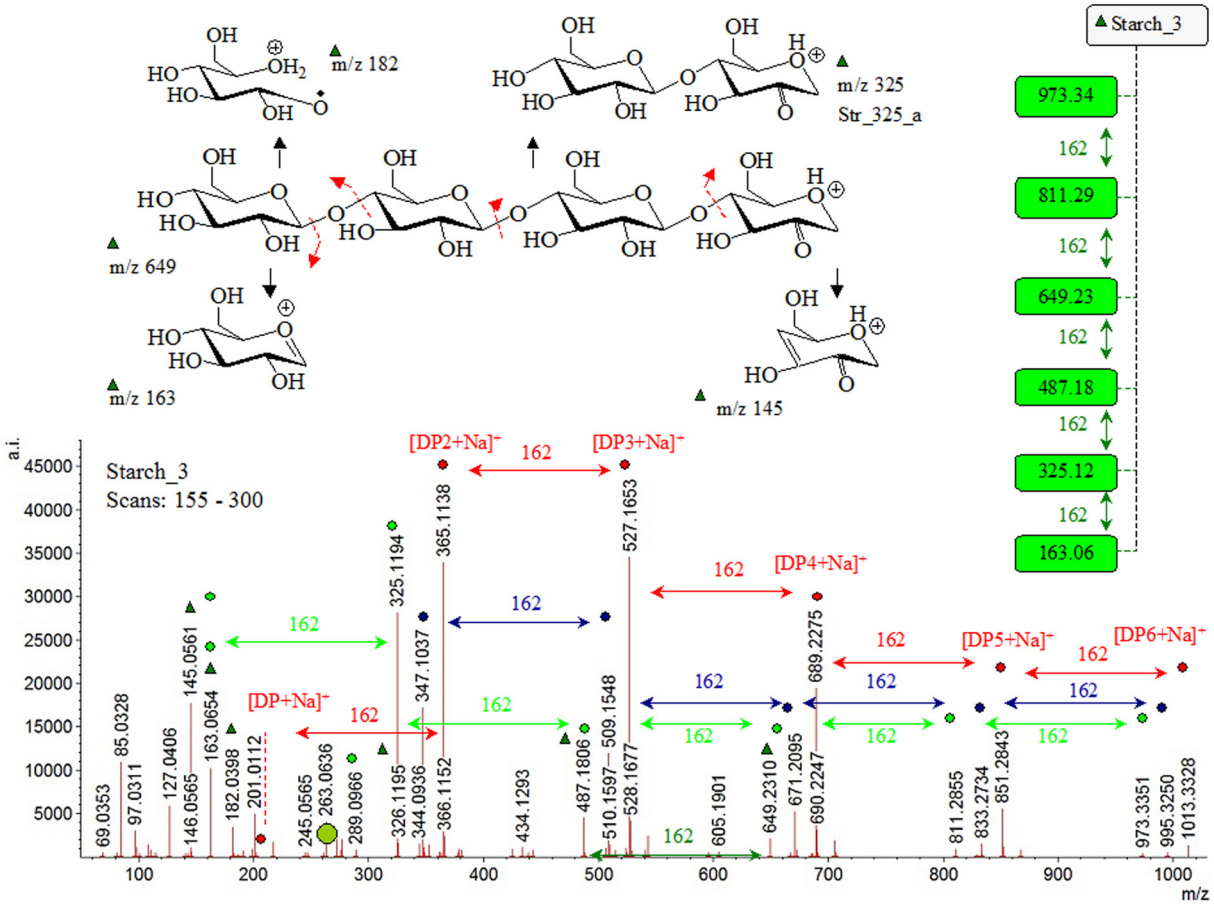

Figure 2. Mass spectrum of Starch_3 biopolymer within RT=1.68-3.24min; chemical diagrams of product ions.

furthermore, the abundance of product MS ions within the low m/z values of CBs appears sensitive toward analyte isomers; thus, examining intensity ratio of common MS peaks at m/z 181/180, 162/163, 145, 127, 91, and 85.

Since, the approach is common in quantitative mass spectrometry there are discussed results from analysis of standards. Through, the methods are proven in various fields of analytical mass spectrometry, as well. Thus, we shall explore rigid standard data on testing and assigning results from MS peak intensity values of CBs in starch polymers, because of as sample Starch_3 within 977-1,000 and 920-950 scan numbers show there are abundance peaks at m/z 183.1072, 167.0068, 149.0252, 129.0603, and 83.0524, respectively. The same is valid to Starch_3 and Starch_5 samples (scan numbers 165-186 and 18-31) showing peaks at m/z 182.0398, 163.0654, 145.0509, 126.9521, 97.0311, and 85.0328, respectively. Intensity data on ions at m/z 182, 163, and 85 allow to distinguish among Glc, mannose, and galactose, since linear correlation between MS parameters shows |r|=0.7201 (Glc/Man) and |r|=0.4191 (Glc/Gal) (Figure S15). The figure reveals chemometrics parameters of analysis of intensity of product ions and results from Starch_5 (RT=1.72-1.86min). The highest performance is achieved assessing Starch_5 results with intensity data on mannose (|r|=0.9936.) The study of intensity ratios of peaks I^{97}/I^{127}, I^{127}/I^{145}, and I^{145}/I^{163} of common ions at m/z 97, 127, 145, and 163 show the following data on Starch_5 sample: I^{97}/I^{127}=1.1875, I^{127}/I^{145}=0.66914, and I^{145}/I^{163}=2.3709. The former ratio agrees-well with results from D-glucose[63] showing I^{97}/I^{127}=1. The data on ratio I^{127}/I^{145} =0.66914 correlate-well with result from mannose (I^{127}/I^{145}=0.6.) The value I^{145}/I^{163} =2.3709, however is different from data on three standard samples of carbomonohydrate showing value within 0.22-0.6.

Therefore, study of a statistically representative set of ions of starch within m/z =0-200 indicates that a reliable assignment of species of starch polymer cannot be assured by experimental evidences based on only data on carbomonohydrates; furthermore, evaluating relative intensity data without to account for fluctuations of measurable variables. The major reason for the latter statement is based on the fact that there are examined CBs oligomers in mixture. Due to the latter reasons there is needed to explore a variety of methods in order to provide warrant for a reliable structural assignment of CBs in complex polymers; moreover, it becomes obvious that differentiation of CBs isomers is a challenge, due to diversity of molecular structures of compositions, type of glycoside linkages, and a lot of anomeric configurations.

Despite, available MS approaches to discriminate CB

isomers there are scarce data on quantitative analysis, so far. Method for relative quantification of dimers of CBs based on pairs of analyte ions has been developed. The work in-depth examines affect of type of glycoside linkage on intensity values of characteristic peaks of CBs, including cellobiose, maltose, lactose, gentiobiose, isomaltose, melibiose, laminaribiose, nigerose, and sucrose; thus, encompassing bonding types Glc-β-(1→4) Glc, Glc-α-(1→4)Glc, Gal-β-(1→4)Glc, Glc-β-(1→6) Glc, Glc-α-(1→6)Glc, Gal-α-(1→6)Glc, Glc-β-(1→3)Glc, Glc-α-(1→3)Glc, and Glc-α-(1→2)Fru, respectively. There are assessed common peaks at m/z 143, 161, 179, 221, 263, 281, 291, and 341 by pairs of binary CBs mixtures.

At this point, it is important to emphasize that the study deals with unknown mixtures of oligomers of cellulose- and starch-based polymers in addition to their degradation products; furthermore, they show a similar set of ions within low m/z values. Thus, there is needed to provide a description of advantages of Equation (2) in order to underline its great applicability to determine significantly complex mixtures of structurally very similar analytes at an excellent-to-exact reliability. In the latter context there is one very important fact to highlight, as well. In correlating intensity parameters of MS peaks of discussed analytes toward data on cellobiose (Figure S16), there is achieved |r|=0.97936-0.95118 (Figure S17) Highest parameter value is obtained assessing data on cellobiose and lactose showing |r|=0.97936. Thus, in order to assign reliably structural units of these significantly complex mixtures of analytes it should be bear in mind that analysis of data on Equations (2) and (3) should yield to higher value than |r|=0.979, particularly determining oligomers containing Glc-β-(1→4)Glc and Gal-β-(1→4)Glc type of glycoside-linkage.

Importantly, the results from the same characteristic ions of cellobiose and maltose show |r|=0.14626. The value indicates a significantly reliable determining of isomers of CBs containing Glc-β-(1→4)Glc and Glc-α-(1→4)Glc bonding modes.

Fragment pattern of Glc-β-(1→4)Glc and Glc-β-(1→6) Glc isomers is used to assess data on cellobiose and gentiobiose. MS peaks at m/z 163, 221, and 251 are identical structurally species (Figure S18). Ion at m/z 281 reflects different tautomer. Only, peak at m/z 179 is characterised by significant difference in molecular structure. Due to the latter reason as experimental data clearly show, there is observed difference in intensity value of MS peak at m/z 179 of cellobiose and gentiobiose.

MS/MS pattern of Na^+-adduct of disaccharide at m/z 365.22 shows species at m/z 305.17, 245.03, and 185.07. MS spectrum of sample Cell_3 reveals peaks at m/z 201.0112, 188.9224, 158.9074, 132.1076, 112.9251, and 90.9809, common to cellotriose and strachyose. Thus, intensity data on the latter biopolymer are correlated with values of standard cellotriose and strachyose, showing $|r|=0.4950_4$ and $|r|=0.0774_6$. MS peak at m/z 202 is assigned to sodium adducts of α-cellulose monomer.

Analogously, MS spectrum of Starch_5 reveals peaks at m/z 203.0583, 189.0184, 161.032, 159.0003, 131.0213, 119.0204, 112.9947, 101.0089, and 72.9401. The correlation of intensity data on peaks of species with the values of standard cellotriose and strachyose indicates low mutual correspondence (|r|=0.09625 and 0.07191), while relation of intensity parameters of peaks of samples Cell_3 and Starch_5 yields to |r|=0.75123-0.81202 depending on span of scan time.

Samples Cell_3, Starch_3, and Starch_5 reveal virtually identical ions at m/z 365.114, 527.165, and 689.227, as well. The mutual correlation among intensity data on peaks between pairs of analytes show |r|=0.8406-0.99622 with and without to account for MS sub-peaks of isotope shapes (Figure 3).

Best performances are obtained evaluating Cell_3 and Starch_3 intensity data on peaks at m/z 833.27, 671.21, 509.16, and 347.10 (|r|=0.99622) without to account for molecular isotopomeric peaks. The same is valid to intensity data on peaks at m/z 365.11383, 366.115, 527.165, 528.168, 689.225, and 690.225 of Cell_3 and Starch_3 showing $|r|=0.9993\text{-}0.9970_8$ without and with accounting for sub-peaks of molecular isotopomers. The correlation between species of Starch_5 and Starch_3 shows $|r|=0.8039_2$ and; thus, the discussed CBs dimers and oligomers of cellulose in Cell_3 and Starch_3 can be regarded as identical, due to excellent performances. There is explicit remarks on that the fragmentation pattern is typical for both β-1,4 and α-1,4-linked CBs units[59].

Looking at analysis of thermal degradation of starch and cellulose, there is highlighted structurally very similar MS pattern showing a series of ions at m/z 242.58, 323.61, 485.15, 647.2, 609.26, and 971.31 (starch) as well as m/z 485.15, 647.2, 809.26, and 971.31 (cellulose). The peak spacing is Δ(m/z)=162. Peaks at m/z 242.58, 323.61, 485.15 of starch are assigned to analyte dianions, while cellulose reveals only singly charged anions. However, analogous MS pattern is observed looking at spectra of Starch_3 and Starch_5. Due to the observable similarity of MS spectra of starch and cellulose there has been assigned only their α-(1-6) and β-(1-4) glycoside modes. To products of cellulose decomposition there have been assigned sub-units of type 4,5-dihydroxy-6-hydroxymethyl-dihydro-furan-3-one type of monomeric unit (cation Str_323_a). A loss of 37 Da yields to CBs derivative ending with 1-(3-hydroxy-furan-2-yl)-ethanone fragment. Thus, we assign the MS peak in Cell_3 at m/z

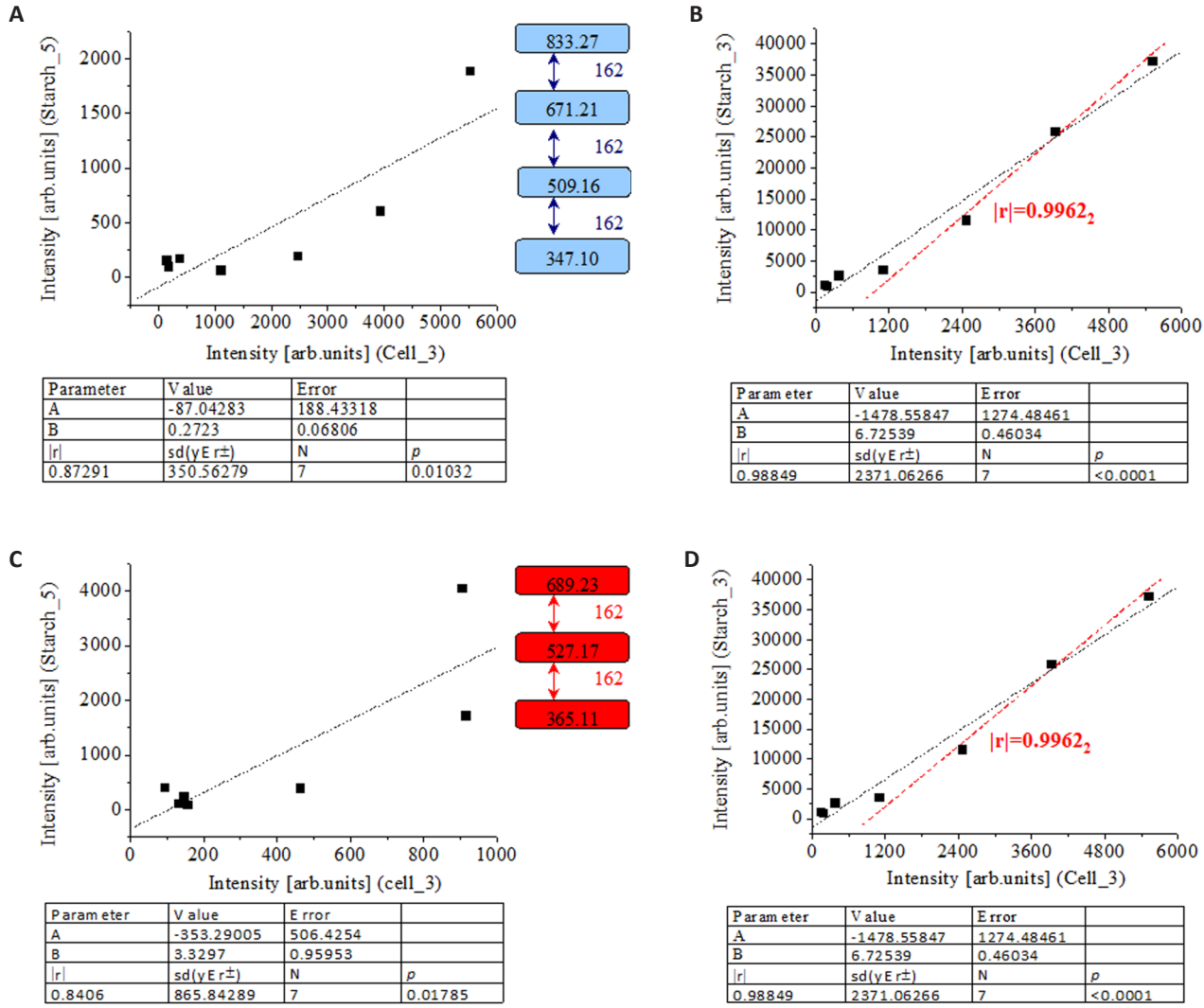

Figure 3. Linear relationship between intensity data (arb.units) of common mass spectrometric peaks of carbohydrates of Cell_3, Starch_3, and Starch_5 samples. Depending on the type of the carbohydrate analyte at m/z 833, 671, 509, and 347 (A,B) and m/z 689, 527, 365 of ions $[M_4+Na]^+$, $[M_3+Na]^+$, and $[M_2+Na]^+$ of Figures 2 and S8 (C, D); there is correlated intensity data on the shown ion *per* pairs of samples Starch_5/Clle_3 (A), Starch_3/Clle_3 (B), Starch_5/Clle_3 (C), and Starch_3/Clle_3 (D) determined per span of scan times; thus, assessing structural changes of biopolymers corresponding to different RTs; chemometrics.

288.9260 to ion Cell_288 (Figure S11).

Cell_3 and Starch_5 reveal a set of common peaks within low m/z values. These are species at m/z 150, 144, 142, 126, 120, 119, 115, 114, 107, 98, 97, 96, 89, 84, 72, 71, 70, 68, and 43, as well[29]. The same is true for cellulose and hemicellulose, showing similar fragmentation patterns and peaks at m/z 217, 201, 185, 163, 151, 139, 127, 111, 97, 83, 64, and 57 (cellulose) as well as at m/z 205, 191, 177, 167, 153, 139, 125, 111, 94, 81, 69, 55, and 44 (hemicellulose). MS peaks at m/z 163, 162, 145, 133, 126, 119, 115, 102, 97, 91, and 85 are associated with ions of 3,6-anhydro-D-glucose [143,144]. MS peak at 114 is cellulose characteristic ion, while ion at m/z 144 is assigned to 1,4;3,6-dianhydro-glucopyranose.

Thus, ions, having peaks at m/z 175, 159, 143, 127, and 95 are assigned to anhydrous-hexosides. MS peaks at m/z 103 and 101 are typically found in mass spectra of methylated anhydrous-hexosides. Disaccharide ions of 3,6-anhydro-L-galactosyl-D-galactose are identified due to spacing of m/z 306.1. Their monosaccharide units show peaks at m/z 144.04 and 180.04. MS ion at m/z 180 is found in lignin mass spectra, as well.

Abundance peaks at m/z 705.5122 and 546.4894 having spacing Δ(m/z)=160 can be assigned to C^1-oxidized oligosaccharides (m/z +16) looking at oxidation reactions of cellulose. MS peaks at m/z 705.2236 and 543.0605 are assigned to sodium $[DP4+16+Na]^+$ and $[DP3+16+Na]^+$ adducts, however, peak at m/z 705 can be assigned to C^4-gem-diol of cellulose tetramer, as well. Due to the latter reasons, the MS fragment pattern indicates, a rather co-existence of different oxidised forms of cellulose oligomers, including a gem-diol one as well as aldonic acid form at reducing end. Non-oxidised fragment species of cellulose are also observed.

The C^1-oxidized product of cellulose oligomers is assigned to disodium adducts as followings: m/z 727.4974 ($[M_4+2Na-H]^+$), 709.21 ($[M_4+2Na-H_2O]^+$),

565.3593 (Y_3), 551.5090 ($^{2,4}A_4$-H_2O), 529.4725 (C_3), 509.1532 (B_3), 467.2181 ($^{0,2}A_3$), 402.5182 (Y_2), 365.1639 (C_2), and 304.8507 ($^{0,2}A_2$), respectively. It agrees well with results from MS analysis of C^1-oxidized cellulose oligomers. Peaks at m/z 707 and 365 belong to sodium adducts of cellobiose dimer and monomer, but owing to the fact that non-covalent bond interacting addicts of oligomers such as [M2+M3+Na] + and $[M_2+M_4+Na]^+$ ones can be proposed, as well as; thus, highlighting the fact that identification of C^1-, C^4-, and C^6-oxidised CBs does not represent a straightforward task. Various analytical tools have been developed for this purpose.

Challenging is determination of C^1- or C^4-oxidation products of cellulose oligomers, due to their elution time. Determination of only m/z data does not capable of distinguishing between C^1- and C^4-oxidised oligosaccharides; thus, highlighting the research task as far from easy one.

The oxidation of C^1-centre of CBs causes for forming of labile δ-lactones; thus, further producing in water aldonic acids[30] (Figure S19). The analytes can be well-separated by high performance anion exchange chromatography.

Conversely, C^4-oxidation reactions of CBs produce 4-keto-aldoses lead to hydrates or germinal diols. C^4-oxidized oligosaccharides undergo tautomerization in alkaline conditions and that limits their analysis by commonly used high performance anion exchange chromatography, despite the fact that there has been questioned whether double oxidised cellulose products are C^1/C^4, or C^1/C^6 oxidised ones[64,65].

MS cannot distinguish isomers and geminal diol of C^4-oxidised products of the oligosaccharide. The C^1-oxidised CBs have equal m/z values. To overcome these challenges there is often used chromatography coupled to mass spectrometry. Despite, there is a lack of a systematic analysis of MS/MS patterns of separated *via* chromatography C^1- and C^4-oxidised CBs[65].

Low abundance peaks at m/z 363.0653, 344.5957 (B_2-H_2O), 321.06 (A_1), 217.9940 (C_1), 202.0149 (Y1), 201.0112 (B1), and 198.9745 of Cell_3 is assigned to geminal diol of cellulose oligomer in agreement with data on oxidised derivatives of the discussed CB[65].

Identification of C^1- and C^4-oxidised CBs structures is far from straightforward as well as; thus, causing for developing of various analytical approaches[66]. Products of oxidised in C^1-centre CBs are lactones that spontaneously convert to aldonic acids. Derivatives C^4 are 4-keto-CBs which spontaneously convert to gem-diols. Derivatives, showing both the C^1- and C^4-oxidised CBs lead to complex mixtures. Elucidation of their biosynthesis and enzymatic degradability is essential for their use to food and non-food industry. Therefore, in-depth structural analysis of their precise 3D molecular structure is essential.

Mass spectrometric data on starch and cellulose standards show MS peaks having spacing Δ(m/z)=162 at 1295.4191, 1133.36, 971.31, 809.26, and 647.2, respectively[26]. The ion at m/z 485.15 is doubly charged in former CBs, while it is monocation of cellulose spectrum. Starch is characterised by two dicationic MS peaks at m/z 323.61 and 242.58, as well.

The sample of Starch_5 exhibits a series of MS peaks having spacing of Δ(m/z)=162. The ions at m/z 671.2095, 509.1548, 433.1324, *etc.,* are characteristic ones of α-CD (m/z 671.20, 509.15, and 347.11) assigned to B_4-B_2 MS cations. The assessment of intensity data on the species comparing with standard of α-CD shows |r|=0.68625. The I_{av}^{exp} values of starch_5 sample are as following: m/z 671.2095 (173.2), 509.1548 (158.4) and 347.1037 (198.8.)

The MS peaks at m/z 365.1138, 527.1653, and 689.2273 are assigned to sodium adducts of cellobiose, cellotriose, and cellotetraose, i.e., $[M_2+Na]^+$, $[M_3+Na]^+$, and $[M_4+Na]^+$ as already shown. It is in agreement with results from work studying ions at m/z 365.11, 527.3, and 689.4 of alkali metal ion adducts of cellobiose oligomers. The MS peak spacing is Δ(m/z)=162, as well. Virtually identical MS pattern can be found in Starch_3 together with common peaks having spacing Δ(m/z)=162 at m/z 347.1037, 509.1548, and 671.2095.

The sample of Starch_3 within the discussed spans of scan time shows peaks at m/z 325.1194, 487.1806, and 649.2310 having spacing Δ(m/z)=162. The peaks are assigned to cellulose. Study of dextran MS spectra shows $[M_n+Na]^+$ adducts at n =2-6 at m/z 365.1024, 527.1568, 689.2103, 851.2630, and 1,013.3145, respectively. It is characterised by α-1,6-glycosidic linkage. Due to these reasons assignment of MS peaks of Starch_3 and Starch_5 includes species of different types accounting not only for presence of alkali metal ion or different proton accepting position of oligomers, but also for type of glycoside chemical bond between monomeric sub-units. MS pattern of ion of Na^+-adduct of CB at m/z 365.22 yields to product species at m/z 305.17, 245.03, and 185.07. In the case of two starch samples there are assigned ions at m/z 301.0081, 247.0417, and 182.0398, respectively. Starch_3 and Starch_5 shows peaks at m/z 245.0565 and 185.0378, while, only, Strach_5 is characterised by peak at m/z 305.0879.

3.2.2 Mass Spectrometric Data on PLA

The MS spectrum of Starch_6 (scans 1,000-1,005) reveals peaks at m/z 145.0509, 217.0735, 289.0966, 361.1219, 433.1387, 505.1645, and 577.1884, having

spacing of Δ(m/z)=72. The anhydrous-hexose unit shows Δ(m/z)=144, while MS reactions associated with loss of monocation of Glc-unit shows peak spacing Δ(m/z)=162[67]. CBs dictations reveal spacing of Δ(m/z)/2[68]. The statement agrees with analysis of multiply charged species of dexran, showing peak spaced Δ(m/z)=162 of singly charged oligomers; Δ(m/z)=81 of dictations of analyte; Δ(m/z)=54 of trications: and Δ(m/z)=40 of quadruplet attachment/charged species, respectively. Due to these reasons starch_6 ions listed above could be assigned to oligomer species of dictations of anhydrous-hexose. Dehydrated oligomers of D-glucose have been found as predominant CBs derivatives of thermally treated cellulose. Formation of 1,6-anhydroglucose at reducing terminal position of oligomers is mainly determined and comparative analysis of MS spectra of cellulose and starch has shown that former CBs stabilises dictations of oligomers, while cellulose species are mainly monocations.

However, MS peak spacing Δ(m/z)=72 is typically observed in samples of PLA[69]. Thus, peaks at m/z 145.0509, 217.0735, 289.0966, 361.1219, 433.1387, 505.1645, and 577.1884 of Strarch_6 can be assigned to PLA ions (Figure 4) accounting for distinguishable cyclic and linear product ions (Figure 5, Figure S21 and S22). Lactide (m/z 145) is highlighted as most stable observable experimental form of PLA[70]. Its D-, L-, and *meso*-forms are accounted for, as well.

Methodological developments of mass spectrometric methods for determining PLA in environmental samples has resulted to MS based quantitative approach to determine the discussed analyte in environmental samples and biological fluids; thus, yields to chemometric method performances r^2=0.9921[69].

3.2.3 Mass Spectrometric Data on Xylo-oligosaccharives

The mass spectrum of Strach_6 sample reveals a set of MS peaks having peak spacing Δ(m/z)=130 (Figure S20) in addition to MS peaks of PLA product ions, discussed above. MS fragment patterns of sodium adducts and neutral species of xylo-oligosaccharives shows abundance ions of ammonium adducts at m/z 608 (Xyl_3GlcA) and 476 (Xyl_2GlcA), having peak spacing Δ(m/z)=132. The peaks at m/z 622 and 490 can be assigned to $Xyl_3MeGlcA$ and $Xyl_2MeGlcA$ oligomers, showing Δ(m/z)=132. The MS peaks at m/z 828, 696, 564, and 432 can be assigned to xylo-containing hexa-, penta-, tetra-, and tetra-mers. MS spectra of sodium adduct of xylo-oligosaccharides produced by partial acid hydrolysis are characterised by peak spacing Δ(m/z)=132 of monocations, while doubly charged product ions of the same type oligomers show Δ(m/z)=66.

Due to similarity of MS pattern of Starch_6 sample and data on xylo-oligosaccharides, the MS peaks at m/z 604.8036, 474.8429, 344.8792, and 214.9248 are assigned, in this study to ammonium adducts of Xyl_3GlcA, Xyl_2GlcA, XylGlcA, and GlcA ions, respectively. The ion at m/z 97 is assigned to 2-furaldehyde. There is current debate on mechanistic aspects of formation of 2-furaldehyde from xylose involve a degradation path D-xylose showing consecutive reactions of acyclic form of xylose, and, thus, producing 1,2-enediol. There are three dehydration steps to obtain the final species. A mechanism involves, again, D-xylose, however acid-catalysed reaction is obtained pyranose. There is a loss of water molecule and intramolecular rearrangement; thus, yielding to 2-furaldehyde, as well.

Owing to that Starch_6 is a starch composite polymer observation of Xyl-containing oligomers assumes a chemically transformed dehydration product of CBs, which is important chemical reaction for the CBs material. It is particularly important for production of biodegradable polymers from biomass. It has been detailed on, *via* high accuracy computational quantum chemical approaches[71]. A correlative analysis with MS data has been performed, as well.

Xylo-oligosaccharides show prospective application to human nutrition, due to their suitable physicochemical properties; for instance, high water solubility, low viscosity, tolerance to high acidic pH and temperature[72]. They are also characterised by a variety of pharmacological functions such as anti-inflammation and anticancer activity, antimicrobial properties, and more.

3.3 Theoretical Data

3.3.1 Calculation of Stochastic Dynamics Parameters

Following the chemometrics tests of identifying statistically equal datasets of MS measurable variables per studied a set of spans of scan time we must begin with data on variables assigned as mutually identical ones, which evaluate statistical significance of data on peaks at m/z 347, 509.2, and 671.2 observed in both the Starch_3 and Starch_5 samples within scan numbers 18-31 and 161-186 (Figure S8). The samples reveal peaks at m/z 347.10367 and 347.16058 (Starch_3) as well as at m/z 347.10367, 347.16058, 347.09552, and 347.0874 (Starch_5); thus, yielding to m/z 347.10841±0.01643 (Starch_3) and 347.14364±0.058 (Starch_5).

Despite, the fact that there is difference in performances looking at standard deviations of data-sets of variables, ANOVA tests (Table S2 and Table S3) show that they are statistically not significantly different. The same is valid to variables at m/z 509.16707±0.0288 (Starch_3) and 509.16982±0.02999 (Starche_5) as well as values of MS peak at m/z 671.20953±0

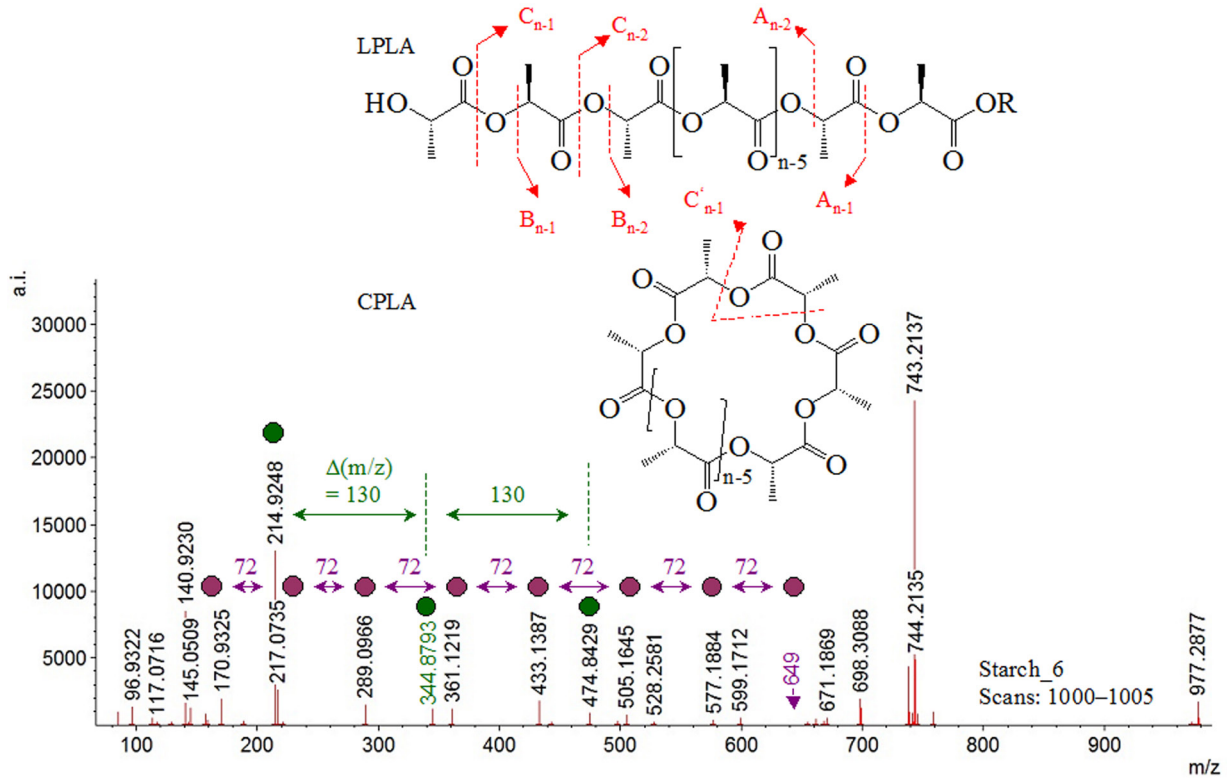

Figure 4. Mass spectrum of sample Starch_6 within RT=13.73-13.77min; chemical diagrams of PLA linear and cyclic ions.

(Starch_3) and 671.22271±0.06501 (Starch_5). They are statistically mutually equal. The discussed product ions of CBs analyte found in two independent samples of biopolymers at m/z 347, 509, and 671 can be defined as equal mutually *per* pairs of datasets of variables and; thus, these species can be regarded as identical structurally.

The important methodological point in the latter context is that there is a lack of theoretical freedom to identify common product ions to the same ionic structure of analytes without assessment of equality of variables over a span of scan time. The theoretical procedure calculating D''_{SD} parameters of Equation (2) in this article uses rigorous statistics tests evaluating identical datasets of MS measurable variables.

If we concentrate on data on m/z 145 in Starch_3 and PLA_01 (Table S4 and Table S5), then the datasets at m/z 145.05614±0 and 145.05089±0 are assigned as two different types of 3D molecular structures of ions having mass 145 Da, because of the experimental variables per span of scan time are statistically significantly different according to ANOVA tests (Table S3).

3.3.2 Calculation of Arrhenius's D_{QC} Parameters

The sub-section discusses computational data on MS species of oligomers in GSs and transition states (TSs), because of the 3D molecular and electronic structure of the MS parent and product ions are characterized by their unique energy parameter (free Gibbs energy) and vibrational modes. Due to the latter reasons the results from frequency analysis of ions in GSs and TSs are accounted for in calculating parameters of Equations (3) and (4). At this point, there is a logic question whether the theoretical method effect on the parameters of the latter equations, because of there is a great variety of theoretical methods showing a variety of accuracy and computational cost. In the latter context the study stresses the reader attention over universally applicable approaches to obtain global minimum of PES and, thus, ground state energetic and vibration modes in addition to BOMD. As can be expected depending on the complexity of the molecular and electronic structures of the species there should be accounted for 3D molecular conformations, electronic effects of tautomerism, inter- and intramolecular charge transfer, intermolecular rearrangement, and more. Due to the latter reasons the content of this sub-section details on few of molecular objects used as examples in order to get sense of difficulties which can be faced studying complex CBs species. The complexity of the molecular structures of CBs, however does not affect on the accuracy of the presented data obtained via balancing between the computational accuracy of the methods and cost of computations and the discussed in this sub-section approaches succeed in describing molecular systems within the framework of Equations (3) and (4). The data on the computed species are summarized in Tables S6-11 detailing on energetic of ions in GS and TS; their atomic co-ordinates, together

with vibration modes. The first stage of computations provides most stable MM2/MD geometry of species (Figure S23), while next, stage accounts of molecular optimisation of geometry from stage one. However, there is used high accuracy level of theory. The TS is studied via Born-Oppenheimer MD (Figure S24). The results from computations and methods, having different accuracy such as MM2/MD and DFT ones yield to energy parameters of species which are linearly correlation. The analysis of energy parameters of species assigning to MS peak at m/z 325 of cellulose dimer, i.e. Cell_325_a, Cell_325_b, and Cell_325_c of MM2/MD and M062X/SDD methods show |r|=0.99972 (Figures S25, S26). The latter result is important, because of frequently the reader's attention focuses on data on high accuracy methods in describing 3D molecular geometry and conformations of molecular systems. The results from the latter figure highlight that the former approach provides qualitatively identical data. The statement is associated with the fact that we always find in puzzling how we should describe 3D molecular conformations of MS observable oligomers of CBs where employment in high accuracy computations fails to provide balanced view between accuracy and computational cost. Figures S23-26 assume that MM2/MD data on low costs theoretical optimisation provide reliable description of 3D molecular structure of oligomer and polymer ions. There is variation of exact energy and geometry parameters of species depending on theoretical methods. An ambiguous assignment could be possible studying very large CB-systems.

Despite the latter comment on M062X/SDD has shown highly reliable assignment of not only molecular geometry of species, but also subtle electronic effects. It is proven as really reliable method, examining tautomers of organics. Data on aforementioned figures reveal that in case of cation Cell_325_c there is intramolecular proton and charge transfer effects causing for formation of macrocyclic structure of ion with OH^+ proton localisation instead of CH_2^+-one. There is decreasing in energy of ionic system. Ion Cell_325_c is characterised by lowest ΔG-parameter of GS within the studied series of ions assigning to MS peak at m/z 325.

The results presented above support a two-fold conclusion: (1) In assigning CBs oligomeric MS peaks there should be accounted for a variety of molecular ions depending protomer; and as aforementioned (2) each of the ions can have its own characteristics depending on molecular structures; thus, causing for charge transfer effects, as well. All these intramolecular effects contribute crucially to vibration modes of MS ions. Due to the latter fact there should be accounted for them precisely in order to provide accurate assignment of experimental MS ions to corresponding 3D molecular conformation and electronic structure of species. There is relative complexity of the molecular computations of MS observed species, however, Equations (3) and (4) offer a crucial alternative involved into MS based structural analysis, because of they account for molecular structure, geometry parameters, and chemical reactivity of species *via* computations of vibration modes in global minimum of energy or the most stable molecular geometry of ion and its transition state. In order to complete the examples of molecular species discussed in this sub-section toward their class of ogranics, MM2/MD data on PLA fragment ions are shown as Figure S27, as well.

3.4 Correlative Analysis between Experimental and Theoretical data

Looking at D_{QC} and I_{SD}^{Theor} data on ions of MS peaks of Starch_3 together with experimental D''_{SD} parameters of Equation (2) (Table S4), we have a whole set of quantities and measurable variables whose purpose is to link truth 3D molecular and electronic structures of observable CBs ions with experimental measurable parameters assessing m/z and intensity measurands. Due to the latter reasons there should be no misunderstanding, regarding capability of Equation (2) of exact distinguishing among 3D molecular structure of CBs species in real complex samples of mixtures of even structurally very similar product ions.

Thus, among studies series of 3D molecular structures of MS peak at m/z 325.11935±0 labelled as $Cell_{\_325\_a}$, $Cell_{\_325\_b}$, $Cell_{\_325\_c}$, and $Str_{\_325\_a}$ belonging to CB-dimers, having different type of glycoside bond and proton accepting position together with isomeric forms, there is achieved excellent performances showing |r|=0.99904 evaluating relation $I_{SD}^{Ther} = f(D''_{SD})$ of D''_{SD} parameters of ions at m/z 325.11935±0, 163.06538, and 145.05614 as well as theoretical results from 3D molecular structure Str_325_a. The analysis of the later relation, however, accounting theoretical D_{QC} results from 3D molecular structures of ions $Cell_{\_325\_a}$, $Cell_{\_325\_b}$, and $Cell_{\_325\_c}$ yields to |r|=0.99899, 0.98841, and 0.99748.

In assessing data on 3D structures of ions of peak at m/z 325, i.e. $Str_{\_325\_a}$ and $Cell_{\_325\_a}$ ones, showing |r|=0.99904 and |r|=0.99899 one needs to be obvious about what great advantages of Equation (2) consists in: It is capable of distinguishing among electronic effects of structurally very similar CB ions at excellent performances, owing to difference in the parameters ΔΔ|r|=0.00005. Discussing further data on ion at m/z 325 it should be said that as Figure 5 reveals both $Str_{\_325\_a}$ and $Cell_{\_325}$ ions show glycoside linkage of monsachharides of β-D-(1→4) type, however, higher |r|-coefficient is obtained assessing parameters of ketone-form of the CBs unit, rather than oxonium cation and with this in view, one can see further that difference in |r|-data on α(1→6) and β(1→4) glycoside bonding isomers of ions $Cell_{\_325\_a}$ and $Str_{\_325\_a}$ is ΔΔ|r|=-0.00156.

Therefore, the Equation (2) is capable of reliable

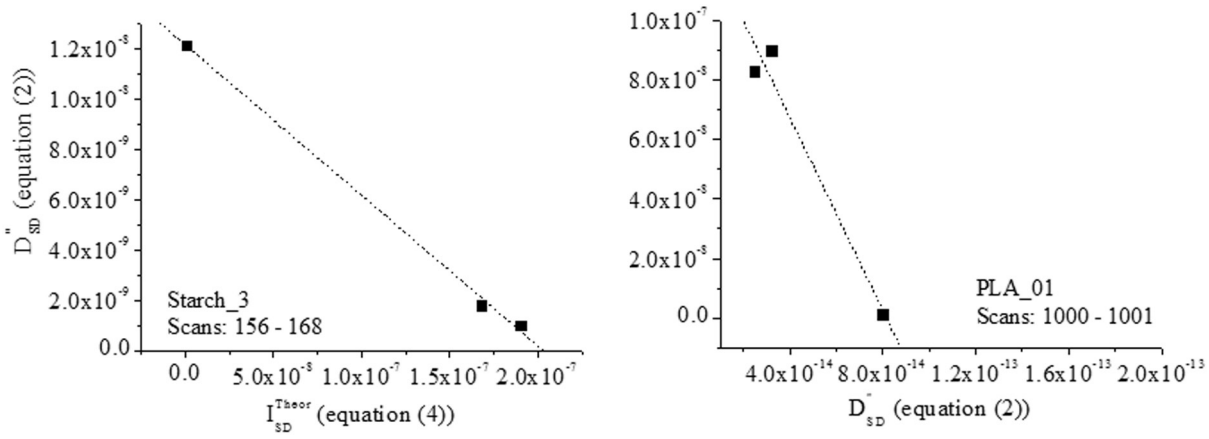

Parameter	Mean	Error	
A	1.213.10^{-8}	3.85336.10^{-10}	
B	-0.05976	0.00262	
|r|	sd(yEr±)	N	*p*
0.99904	3.83612.10^{-10}	3	0.02788

Parameter	Value	Error	
A	1.32023.10^{-7}	1.64133.10^{-8}	
B	-1.61703.10^{6}	314948.05419	
|r|	sd(yEr±)	N	*p*
0.98156	1.3305.10^{-8}	3	0.12246

Figure 5. Linear relation between experimental and theoretical intensity data on Equations (2) and (4) of ions of carbohydrates in Starch_3 and PLA (PLA_01) biopolymers of film of 100% corn starch and single-use drinking cup of fermented corn starch; chemometrics.

distinguishing among glycoside type bonding of CBs dimers and oligomers; thus, determining exactly not only type of CBs oligomers in real mixtures of commercial biodegradable compositions of polymers, but also 3D molecular structures of polymer components. As can be seen as well as Figure 5 depicts linear relation between theoretical and experimental intensity data on PLA, and using results from Table S4 and Tables S9-S11. There is obtained high chemometric method performances, showing |r|=0.98156. The latter result highlights that Equation (2) determines structurally CB components of biodegradable polymers; thus, providing crucial results among already known methods tested, so far. It produces solutions of general problematization that has been made by MS analysis of biodegradable polymers, due to their high complexity and diversity of components.

Assessing the reported for the first time in the literature in this study excellent performances in applying Equation (2) to analyse structurally CBs in biodegradable polymers it appears, in actual fact, new solution of current known problematization of reliable quantitative and structural analysis of biodegradable polymers by routinely implemented MS approaches showing mainly reliability up to |r|=0.99 of semiquantitative analysis; furthermore, proposing mainly 2D structures of parent and product ions.

Thus, the new results, herein, highlight those innovative stochastic dynamics model Equation (2) clearly grasps problematization of structural analysis of components of complex commercial products of biodegradable polymers not only as pro-argument of application of the formula to fundamental research, but as a reliable work of thought.

4 CONCLUSION

The study is mainly concerned with application of innovative stochastic dynamics model Equations (2) and (4) to determine mass spectrometrically components of biodegradable bioplastics looking at PLA in starch containing composite polymers used to food packing industry. The equations have a twofold function in the mass spectrometric analysis. Equation (2) is an exact model for quantitative analysis of complex multicomponent samples of the environment, foods, and biological fluids. It has been already empirically tested[46,47,49]. Its application to determine exactly 3D molecular and electronic structures of biopolymers in complex samples of starch-based food packing commercial materials is tested for first time, herein; thus, studying samples, containing within the 3,479-15,770 chemicals per packing has shown |r|=0.99904-0.98156 looking at analysis of carbohydrates in starch and PLA biopolymers in films of 100% corn starch and single-use drinking cup of fermented corn starch. The excellent performances show that pure concept of stochastic dynamics mass spectrometry and its model Equations (2) and (4) is prospectively applicable not only to analytical practice of fundamental research, but also to industry. The claim has been fruitfully applied to analysis of very complex commercial biopolymer food packing samples, containing unknown carbohydrate, as well. As discussed in preceding sections of the study, due to latter reasons our further attempts are to derive new pro-arguments for universal application of the functional models as exact tools for both quantitative and structural mass spectrometric based analysis to real samples of environment, foods, and biological fluids.

Acknowledgements

The author thanks the Deutsche Forschungsgemeinschaft; Alexander von Humboldt Stiftung; *Deutscher Akademischer Austausch Dienst* for grant within priority program Stability Pact South-Eastern Europe.

Conflicts of Interest

The author declared no conflict of interest.

Data Available

Experimental mass spectrometric and infrared spectroscopic raw-data are publicly available and can be downloaded free of charge (https://zenodo.org/records/4004763). Mass spectrometric, chemometrics, and theoretical data (Supplementary Data).

Author Contribution

Ivanova B conceptualized project idea and set out the project design, collected data, literature survey and writing up the manuscript.

Abbreviation List

BOMD, Born-Oppenheimer molecular dynamics
Ca., Circa
CB(s), Carbohydrate(s)
D_{QC}, Quantum chemical diffusion parameter according to Arrhenius's theory
D_{SD}, Stochastic dynamic diffusion parameters according to our theory
ESI, Electrospray ionization (mass spectrometric method)
FT-IR, Fourier transform infrared (spectroscopy)
GS, Ground state
Gly, D-glucose
I, Intensity of mass spectrometric peak (variable)
LMW, Low-molecular-weight (analytes)
LPLA, Linear polylactic acid
m/z, Mass-to-charge (mass spectrometric variable)
MD, Molecular dynamics
MM, Molecular mechanics
MS, Mass spectrometry
MS/MS, Tandem mass spectrometric operation mode
PLA, Polylactic acid
|r|, Statistical coefficient of linear correlation (chemometrics)
RT, Retention time
TS, Transition state
ΔG, (Difference) in free Gibbs energy

References

[1] Nizamuddin S, Chen C. Biobased, biodegradable and compostable plastics: Chemical nature, biodegradation pathways and environmental strategy. *Environm Sci Pollut Res*, 2024; 31: 8387-8399.[DOI]

[2] Kim M, Chang H, Zheng L et al. A review of biodegradable plastics: Chemistry, applications, properties, and future research needs. *Chem Rev*, 2023; 123: 9915-9939.[DOI]

[3] Zhang H, Su Z, Wang X. Starch-based rehealable and degradable bioplastic enabled by dynamic imine chemistry. *ACS Sustain Chem Eng*, 2022; 10: 8650-8657.[DOI]

[4] Yu Y, Flury M. Unlocking the potentials of biodegradable plastics with proper management and evaluation at environmentally relevant concentrations. *Npj Mater Sustain*, 2024; 2: 9.[DOI]

[5] Dey S, Veerendra G, Babu P et al. Degradation of plastics waste and its effects on biological ecosystems: A scientific analysis and comprehensive review. *Biomed Mater Devices*, 2024; 2: 70-112.[DOI]

[6] Yekta R, Firoozjah R, Salim S et al. Application of cellulose and cellulose derivatives in smart/ intelligent bio-based food packaging. *Cellulose*, 2023; 30: 9925-9953.[DOI]

[7] Aznar M, Ubeda S, Dreolin N et al. Determination of non-volatile components of a biodegradable foodpackaging material based on polyester and polylactic acid (PLA) andits migration to food simulants. *J Chromatogr A*, 2019; 1583: 1-8.[DOI]

[8] Shekhar N, Mondal A. Synthesis, properties, environmental degradation, processing, and applications of polylactic acid (PLA): An overview. *Polym Bull*, 2024; 81: 11421-11457.[DOI]

[9] Gadhave R, Das A, Mahanwar P et al. Starch based bio-plastics: The future of sustainable packaging. *Open J Polymer Chem*, 2018; 8: 21-33.[DOI]

[10] EUR-Lex. European Parliament and Council Directive 94/62/EC of 20 December 1994 on packaging and packaging waste. Available at:[Web]

[11] Jieying S, Tingting L, Caie W et al. Paper-based material with hydrophobic and antimicrobial properties: Advanced packaging materials for food applications. *Compr Rev Food Sci Food Saf*, 2024; 23: e13373.[DOI]

[12] Resolution Adopted by the United Nations Environment Assembly on 2 March 2022-5/14. End Plastic Pollution: Towards an International Legally Binding Instrument. UNEP, 2022. Accessed November 11, 2022. Available at:[Web]

[13] Chia H, Wu B. Recent advances in 3D printing of biomaterials. *J Biol Engin*, 2015; 9: 4.[DOI]

[14] Dana H, Ebrahimi F. Synthesis, properties, and applications of polylacticacid-based polymers. *Polym Eng Sci*, 2023; 63: 22-43.[DOI]

[15] Liu Y, Li N, Zhang X et al. Eco-friendly drinking straws: Navigating challenges and innovations. *Trends Food Sci Technol*, 2024; 148: 104511.[DOI]

[16] Li Y, Wang S, Qian S et al. Depolymerization and Re/Upcycling of Biodegradable PLA Plastics. *ACS Omega*, 2024; 9: 13509-13521.[DOI]

[17] Gupta R, Samantaray P, Bose S. Going beyond cellulose and chitosan: Synthetic biodegradable membranes for drinking water, wastewater, and oil-water remediation. *ACS Omega*, 2023; 8: 24695-24717.[DOI]

[18] Yasien N, Swilam D, Gamil M et al. Chapter 27: Impacts of biodegradable plastic on the environment; In: Handbook of Biodegradable Materials (Ali GA and Makhlouf ASH Eds.). Springer Nature: Cham, Switzerland, 2023.

[19] EUR-Lex. Commission Regulation (EU) No 1935/2004 of the European Parliament and of the council of 27 October 2004 on materials and articles intended to come into contact with food and repealing Directives 80/590/EEC and 8 9/109/EEC. 2004; L338/4-16. Available at:[Web]

[20] EUR-Lex. Commission Regulation (EU) No 2020/1245 of 2 September 2020 amending and correcting Regulation (EU) No 10/2011 on plastic materials and articles intended to come into contact with food. 2020; L288, 1-17. Available at:[Web]

[21] Osorio J, Aznar M, Nerin C et al. Comparison of LC-ESI, DART, and ASAP for the analysis of oligomers migration from biopolymer food packaging materials in food (simulants). *Anal Bioanal Chem*, 2022; 414: 1335-1345.[DOI]

[22] Bastioli C. Properties and applications of Mater-Bi starch-based materials. *Polymer Degrad Stabil*, 1998; 59: 263-212.[DOI]

[23] Chen X, Yan S, Wang H et al. Aerobic oxidation of starch catalyzed by isopolyoxovanadate $Na_4Co(H_2O)_6V_{10}O_{28}$. *Carbohydr Polym*, 2015; 117: 673-680.[DOI]

[24] Riboni N, Bianchi F, Cavazza A et al. Mass spectrometry-based techniques for the detection of non-intentionally added substances in bioplastics. *Separations*, 2023; 10: 22.[DOI]

[25] Tolonen L, Juvonen M, Niemelae K et al. Supercritical water treatment for cello-oligosaccharide production from microcrystalline cellulose. *Carbohydr Res*, 2015; 401: 16-23.[DOI]

[26] Golon A, Gonzalez F, Davalos J et al. Investigating the thermal decomposition of starch and cellulose in model systems and toasted bread using domino tandem mass spectrometry. *J Agric Food Chem*, 2013; 61: 674-684.[DOI]

[27] Barbosa-Nunez J, Espinosa-Andrews H, Cardon A et al. Polymer-based encapsulation in food products: A comprehensive review of applications and advancements. *J Future Foods*, 2025; 5-1: 36-49.[DOI]

[28] Huang Y, Robinson R, Barile D. Food glycomics: Dealing with unexpected degradation of oligosaccharides during sample preparation and analysis. *J Food Drug Anal*, 2024; 30: 6.[DOI]

[29] Xue P, Liu M, Yang H et al. Mechanism study on pyrolysis interaction between cellulose, hemicellulose, and lignin based on photoionization time-of-flight mass spectrometer (PI-TOF-MS) analysis. *Fuel*, 2023; 338: 127276.[DOI]

[30] Frommhagen M, Van Erven G, Sanders M et al. RP-UHPLC-UV-ESI-MS/MS analysis of LPMO generated C^4-oxidized gluco-oligosaccharides after non-reductive labeling with 2-aminobenzamide. *Carbohydr Res*, 2017; 448: 191-199.[DOI]

[31] Global Agricultural Information Network. GAIN Report Number: RS1035. 2010. Available at:[Web]

[32] Ruggero F, Carretti E, Gori R et al. Monitoring of degradation of starch-based biopolymer film under different composting conditions, using TGA, FTIR and SEM analysis. *Chemosphere*, 2020; 246: 125770.[DOI]

[33] Zimmermann L, Dombrowski A, Volker C et al. Are bioplastics and plant-based materials safer than conventional plastics? In vitro toxicity and chemical composition. *Environm Int*, 2020; 145; 106066.[DOI]

[34] Zimmermann L, Dierkes G, Ternes T et al. Benchmarking the in vitro toxicity and chemical composition of plastic consumer products. *Environ Sci Technol*, 2019; 53: 11467-11477.[DOI]

[35] Anna V, Rimma S, Ovadia L et al. GC determination of N-nitrosamines by supersonic molecular beam MS equipped with triple quadrupole analyzer, GC/SMB/QQQ/MS. *Anal Chim Acta*, 2011; 685: 162-169.[DOI]

[36] Binda G, Costa M, Supraha L et al. Untangling the role of biotic and abiotic ageing of various environmental plastics toward the sorption of metals. *Sci Tot Environm*, 2023; 893: 164807.[DOI]

[37] EUR-Lex. Commission Regulation (EU) No 10/2011 of 14 January 2011 on plastic materials and articles intended to come into contact with food Text with EEA relevance. Available at:[Web]

[38] EUR-Lex. Council Directive 96/23/EC of 29 April 1996 on measures to monitor certain substances and residues thereof in live animals and animal products and repealing Directives 85/358/EEC and 86/469/EEC and Decisions 89/187/EEC and 91/664/EEC. Available at:[Web]

[39] Bos T, Pirok B, Karlson L et al. Fingerprinting of hydroxy propyl methyl cellulose by comprehensive two-dimensional liquid chromatography-mass spectrometry of monomers resulting from acid hydrolysis. *J Chromatogr A*, 2024; 1722: 464874.[DOI]

[40] Ivanova B. Special Issue with Research Topics on "Recent Analysis and Applications of Mass Spectra on Biochemistry". *Int J Mol Sci*, 2024; 25: 1995.[DOI]

[41] Wang Z, Liu P, Li L. A tutorial review of labeling methods in mass spectrometry-based quantitative proteomics. *ACS Meas Sci Au*, 2024; 4: 315-337.[DOI]

[42] Wesdemiotis C. Multidimensional mass spectrometry of synthetic polymers and advanced materials. *Angew Chem Int Ed*, 2017; 56: 1452-1464.[DOI]

[43] Wesdemiotis C, Williams-Pavlantos K, Keating A et al. Mass spectrometry of polymers: A tutorial review. *Mass Spectrom Rev*, 2024; 43: 427-476.[DOI]

[44] Zimmermann L, Dombrowski A, Voelker C et al. Raw data for "Are bioplastics and plant-based materials safer than conventional plastics? In vitro toxicity and chemical composition" Zenodo; CERN database repository. Accessed August 27, 2020. Available at:[Web]

[45] Ivanova B, Spiteller M. Experimental and theoretical mass spectrometric quantification of diffusion parameters and 3D structural determination of ions of L-tryptophyl-L-tryptophan in electrospray ionization conditions in positive operation mode. *J Mol Struct*, 2018; 1173: 848-864.[DOI]

[46] Ivanova B. Stochastic dynamic mass spectrometric quantitative and structural analyses of pharmaceutics and biocides in biota and sewage sludge. *Int J Mol Sci*, 2023; 24: 6306.[DOI]

[47] Ivanova B, Spiteller M. Stochastic dynamic electrospray ionization mass spectrometric quantitative analysis of metronidazole in human urine. *Anal Chem Lett*, 2022; 12: 322-348.[DOI]

[48] Upadyshev M, Ivanova B, Motyleva S. Mass spectrometric identification of metabolites after magnetic-pulse treatment of infected Pyrus communis L. microplants. *Int J Mol Sci*, 2023; 24: 16776.[DOI]

[49] Ivanova B. Stochastic dynamics mass spectrometric structural analysis of poly(methyl methacrylate). *Univ J Carbon Res*, 2024; 2: 60-88.[DOI]

[50] Allinger L. Conformational analysis. 130. MM2. A hydrocarbon force field utilizing V1 and V2 torsional terms. *J Am Chem Soc*, 1977; 99: 8127-8134.[DOI]

[51] Miller JN, Miller JC. Statistics and chemometrics for analytical chemistry. Pentice Hall: London, England, 1988.

[52] Akopyan SM, Khachatryan AG. Synthesis of new substituted 2,3-dihydro-1,4-dioxin-2-ones and 1,4-dioxan-2-ones. *Russian J Org Chem*, 2003; 39: 103431036.[DOI]

[53] Kotatha D, Rungrodnimitchai S. Synthesis and characterization of nanofiber of oxidized cellulose from Nata De Coco. *Int J Chem Engin*, 2018; 8: 2787035.[DOI]

[54] Zhbankov R. Vibrational spectra polysaccharides. *J Mol Struct*, 1992; 272: 347-360.[DOI]

[55] Andrianov V, Zhbankov R, Dashevskii V. A theoretical study of the vibrational spectrum of cellobiose within the ramework of the additive model of interatomic interactions. *Z Strukt Khimii*, 1980; 21: 85-90.[DOI]

[56] Ivanova B, Tsalev D, Arnaudov M. Validation of reducing-difference procedure for the interpretation of non-polarized infrared spectra of n-component solid mixtures. *Talanta*, 2006; 69: 822-828.[DOI]

[57] Liu Z, Zhao Y, Wang H et al. Studies on the nano-structures of wheat starch granules using electrospray ionization mass spectrometry. *Ultramicroscopy*, 2005; 105: 287-292.[DOI]

[58] Wang Y, Liu L, Ma L et al. Identification of saccharides by using direct analysis in real time (DART) mass spectrometry. *Int J Mass Spectrom*, 2014; 357: 51-57.[DOI]

[59] Grabarics M, Lettow M, Kirschbaum C et al. Mass spectrometry-based techniques to elucidate the sugar code. *Chem Rev*, 2021; 122: 7840-7908.[DOI]

[60] Castillo J, Galermo A, Amicucci M et al. A multidimensional mass spectrometry-based workflow for de novo structural elucidation of oligosaccharides from polysaccharides. *J Am Soc Mass Spectrom*, 2021; 32: 2175-2185.[DOI]

[61] Dommon D, Costello C. A systematic nomenclature for carbohydrate fragmentations in FAB-MS/MS spectra of glycoconjugates. *Glycoconjugate J*, 1988; 5: 397-409.[DOI]

[62] Rumiantseva L, Osipenko S, Zharikov A et al. Analysis of $^{16}O/^{18}O$ and H/D exchange reactions between carbohydrates and heavy water using high-resolution mass spectrometry. *Int J Mol Sci*, 2022; 23: 3585.[DOI]

[63] Madhusudanan K. Tandem mass spectra of ammonium adducts of monosaccharides: Differentiation of diastereomers. *J Mass Spectrom*, 2006; 41: 1096-1104.[DOI]

[64] Sun P, Laurent C, Boerkamp V et al. Regioselective C^4 and C^6 double oxidation of cellulose by lytic polysaccharide monooxygenases. *ChemSusChem*, 2022; 15: e202102203.[DOI]

[65] Westereng B, Arntzen M, Aachmann F et al. Simultaneous analysis of C^1 and C^4 oxidized oligosaccharides, theproducts of lytic polysaccharide monooxygenases acting on cellulose. *J Chromatogr A*, 2016; 1445: 46-54.[DOI]

[66] Mudedla S, Vuorte M, Veijola E et al. Effect of oxidation on cellulose and water structure: A molecular dynamics simulation study. *Cellulose*, 2021; 28: 3917-3933.[DOI]

[67] Kyselova L, Rezanka T. Analysis of glycosylated cardiolipins from thermophilic bacteria using GC-MS and LC-ESI-MS/MS methods. *J Pharmaceut Biomed Anal*, 2024; 238: 11580.[DOI]

[68] Ivanova B, Spiteller M. Stochastic dynamics mass spectrometric 3D structural analysis of N-glycans of fetal bovine serum - an experimental and theoretical study. *Med Sci Forum*, 2022; 14: 2.[DOI]

[69] Wang L, Peng Y, Xu Y et al. An in situ depolymerization and liquid chromatography-tandem mass spectrometry method for quantifying polylactic acid microplastics in environmental samples. *Environ Sci Technol*, 2022; 56: 13029-13035.[DOI]

[70] Feng L, Cui C, Li Z et al. Kinetics of catalyzed thermal degradation of polylactide and its application as sacrificial templates. *Chin J Chem*, 2022; 40: 2801-2807.[DOI]

[71] Lupi L, Ayarde-Henriquez L, Kelly M et al. Ab initio and kinetic modeling of β-D-xylopyranose under fast pyrolysis conditions. *J Phys Chem A*, 2024; 128, 1009-1024.[DOI]

[72] Chen Y, Xie Y, Ajuwon K et al. Xylo-oligosaccharides, preparation and application to human and animal health: A review. *Front Nutr*, 2021; 8. 731930.[DOI]